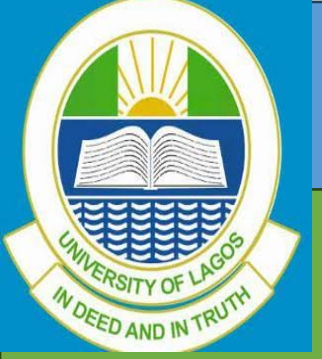

NASA 4th EDDY CROSS DISCIPLINARY SYMPOSIUM

Responses of the African and American Equatorial Ionization Anomaly (EIA) to the 2014 Arctic Sudden Stratospheric Warming (SSW) Events

By

O. R. Idolor[1], A. O. Akala[1], O. S. Bolaji[1], E. O. Oyeyemi[1]

[1] Department of Physics, University of Lagos, Akoka, Yaba, Lagos, Nigeria

Introduction

Background of the study

Previous studies have shown that the variability in the ionosphere during Sudden Stratospheric Warming (SSW) events is connected to the coupling of the lower and upper atmosphere (Goncharenko et al., 2010; 2013).

Understanding of this connection between the lower and upper atmosphere has remained a major concern for the space science community.

SSWs are large-scale meteorological events characterized by the sudden breakdown of the stratospheric polar vortex arising from the dynamic forcing of the upward propagating planetary waves originating from the lower atmosphere (Jonah *et al.*, 2014).

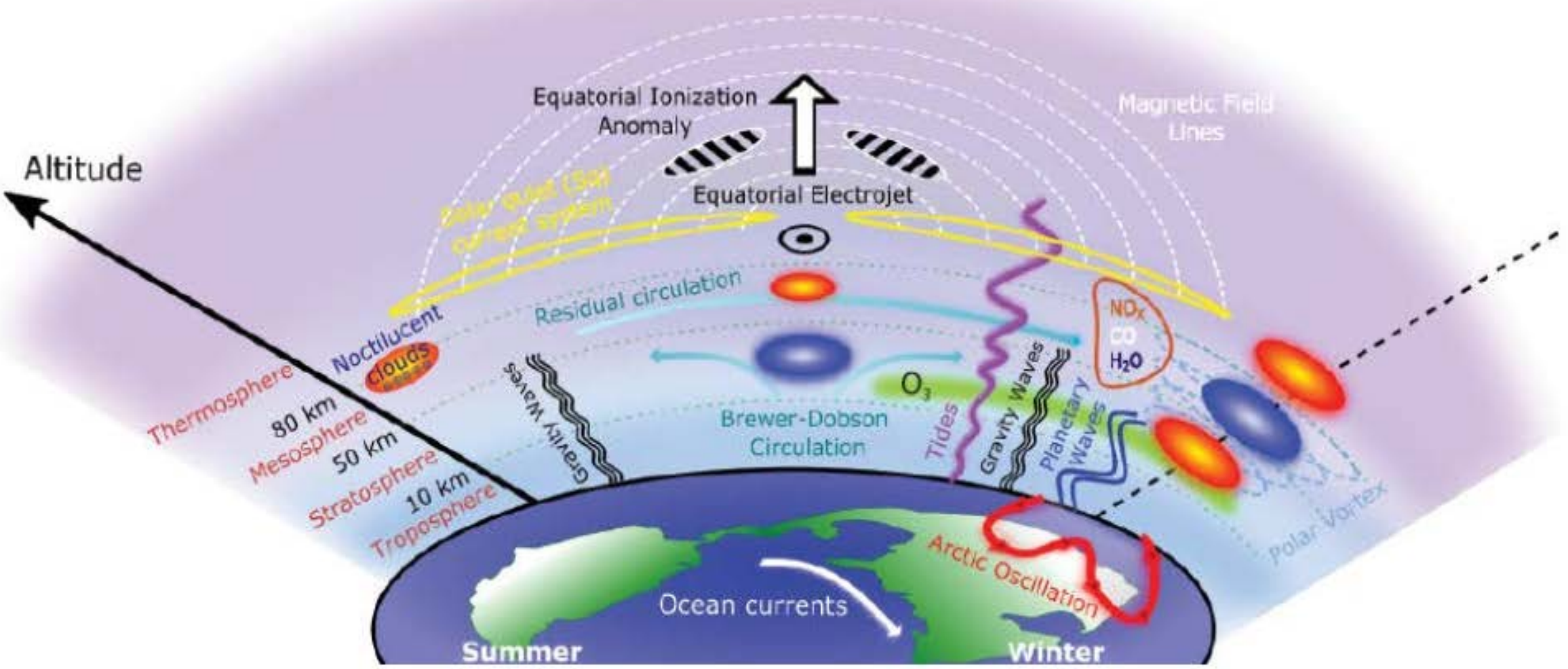

Figure 1: Schematic of the coupling processes and atmospheric variability that occur during sudden stratospheric warming events. Red and blue circles denote regions of warming and cooling respectively (adapted from Pedatella *et al.*, 2018).

SSW events can be classified into major or minor warming. Both major and minor warming events are characterized by the abrupt rise in stratospheric temperature at 90ºN and 10 hPa (Chau *et al.*, 2012).

Several studies have also reported that SSW effects contribute significantly to wide range of climate r extreme surface weather events (Pedatella *et al.*, 2018, Domeisen & Butler, 2020).

These events include cold air outbreak, extreme heat, drought, air pollution, wild fires, among others.

Data and Methodology

Data

The stratospheric temperature and zonal mean wind data was obtained from NOAA web address http://www.esrl.noaa.gov/psd/

The GPS observable data were obtained from the following GPS networks: IGS (www.igs.org), UNAVCO (www.unavco.org), SONEL (www.sonel.org), REGME (http://www.geoportaligm.gob.ec/portal/), and AFREF (www.afrefdata.org).

The magnetic field intensity data were obtained from AMBER magnetometer (http://magnetometers.bc.edu/), INTERMAGNET (www.intermagnet.org), (MAGDAS) (http://magdas2.serc.kyushu-u.ac.jp/) and LISN (http://lisn.igp.gob.pe/data/).

Data ctd

The Dst and Kp indices were obtained from the website of the World Data Center for Geomagnetism Kyoto (http://wdc.kugi.kyoto-u.ac.jp/kp/index.html),

The F10.7cm flux was obtained from the website of the NASA space physics data facility. (http://omniweb.gsfc.nasa.gov/form/dx1.html).

The PPEF for February 18-28, and April 11-15 2014 were obtained using the CIRES model of the university of Colorado (http://geomag.colorado.edu/real-time-model-of-the-ionospheric-electric-fields.html)

Methodology

The underlying TEC variations during the SSW event were evaluated by adopting the methodology of Goncharenko *et al*., 2010.

We defined quiet days as days within the period of investigation, when daily 3-hourly Kp ≤ 3 (ΣKp ≤ 24).

Background TEC is given in equation (1) below

$$\Delta TEC = TEC - TEC_{MEAN\ QDS} \quad (1)$$

where TEC is the day-to-day hourly TEC and $TEC_{MEAN\ QDS}$ is the average TEC data for the quiet days of the period of investigation.

Using equation 1 as a reference the second level TEC deviation associated with the geomagnetic storm overlap with the SSW can be filtered from the TEC arising solely from SSW.

$$\Delta TEC2 = \Delta TEC_{overlap} - \Delta TEC_{ssw} \quad (2)$$

Where $\Delta TEC_{overlap}$ TEC from both phenomena, ΔTEC_{ssw} from solely SSW

Methodology Ctd

This study adopted the geomagnetic storm criteria of a minimum Dst of: -100 nT ≤ Dst ≤ -50 nT for moderate storm, and -200 nT ≤ Dst ≤ -100 nT for major storm (Gonzalez *et al.*, 1994)

The Prompt Penetration Electric Field (PPEF) was estimated using the real time electric field model for geomagnetism developed by the Cooperative Institute for Research in Environmental Sciences (CIRES) of the University of Colorado at Boulder (http://geomag.colorado.edu/real-time-model-of-the-ionospheric-electric-fields.html).

Methodology Ctd

To explore the effects of SSW event on the ionospheric irregularities, the Rate of change of TEC (ROT) expressed in units of TEC/min was computed and the five minutes standard deviation of the ROT to obtain ROT Index (ROTI) (Pi *et al*., 1997). ROTI is expressed mathematically as:

$$\mathrm{ROTI} = \sqrt{\langle \mathrm{ROT}^2 \rangle - \langle \mathrm{ROT} \rangle^2} \qquad (3)$$

where ROT in equation (6) is the rate of change of TEC in TECU per minute using a cut off elevation angle of 30º to screen signals arising from non-ionospheric sources, such as multipath.

Methodology Ctd

The 30 minutes average ROTI ($ROTI_{ave}$) was computed. The $ROTI_{ave}$ is given by the expression below.

$$ROTI_{ave} = \frac{1}{Nsat(0.5Hr)} \sum_{N}^{Nsat(0.5Hr)} \sum_{l}^{k} \frac{ROTI(N,0.5Hr,l)}{k} \qquad (4)$$

where N is satellite number, $0.5Hr$ indicates the 30 minutes interval from 0 UT to 24 UT, $Nsat(0.5Hr)$ is the number of visible satellites within 30 minutes interval, k is the number of ROTI index values available for a given satellite and l indicates the ROTI value for every five-minute. The 30 mins average eliminates noise pikes (Oladipo et al., 2014).

Irregularities threshold levels: $ROTI_{ave} < 0.4$ (no irregularities); $0.4 < ROTI_{ave} < 0.8$ (moderate irregularities); and $ROTI_{ave} > 0.8$ (severe irregularities)

Methodology Ctd

In order to compute the equatorial electrojet (EEJ) current, the solar quiet daily variation (*Sq*) for the pairs of stations in both longitudinal sectors were estimated following the procedure outlined by Rabiu *et al*., 2017.

The daily EEJ current was obtained by subtracting the daily *Sq* data of a station located outside the equatorial region from those of the station within the equatorial region.

$$EEJ = H_{eq} - H_{off\text{-}eq} \qquad (5)$$

where H_{eq} and $H_{off\text{-}eq}$ are the magnetic field intensity for the equatorial and off equatorial stations.

Methodology Ctd

Anderson *et al*. (2004) model was adopted to derived the vertical drift.

$$VD = -1989.51 + 1.002Yr - 0.00022DOY - 0.0222F_d - 0.0282F_a - 0.0229Ap \quad (6)$$
$$+ 0.0589Kp - 0.3661LT + 0.1865\Delta H + 0.00028\Delta H^2 - 0.0000023\Delta H^3$$

where VD is the vertical drift, Yr is the year, DOY is the day of the year, F_d is the daily F10.7 cm solar flux, F_a is the 81-day average value of the adjusted F10.7 cm solar flux, Ap and Kp are the daily and 3 hourly geomagnetic indices, LT is the local time in hours, and ΔH is the difference in the horizontal magnetic field intensity.

Methodology Ctd

The EEJ current for the topside ionosphere was estimated from the scalar magnetic field data on board the swarm satellite using the current inversion technique outlined by Aiken *et al*. (2013).

The EEJ current depicts the height-integrated current density profile measured in milli Ampere per meter (mA/m) (Aiken *et al*., 2015).

Methodology ctd

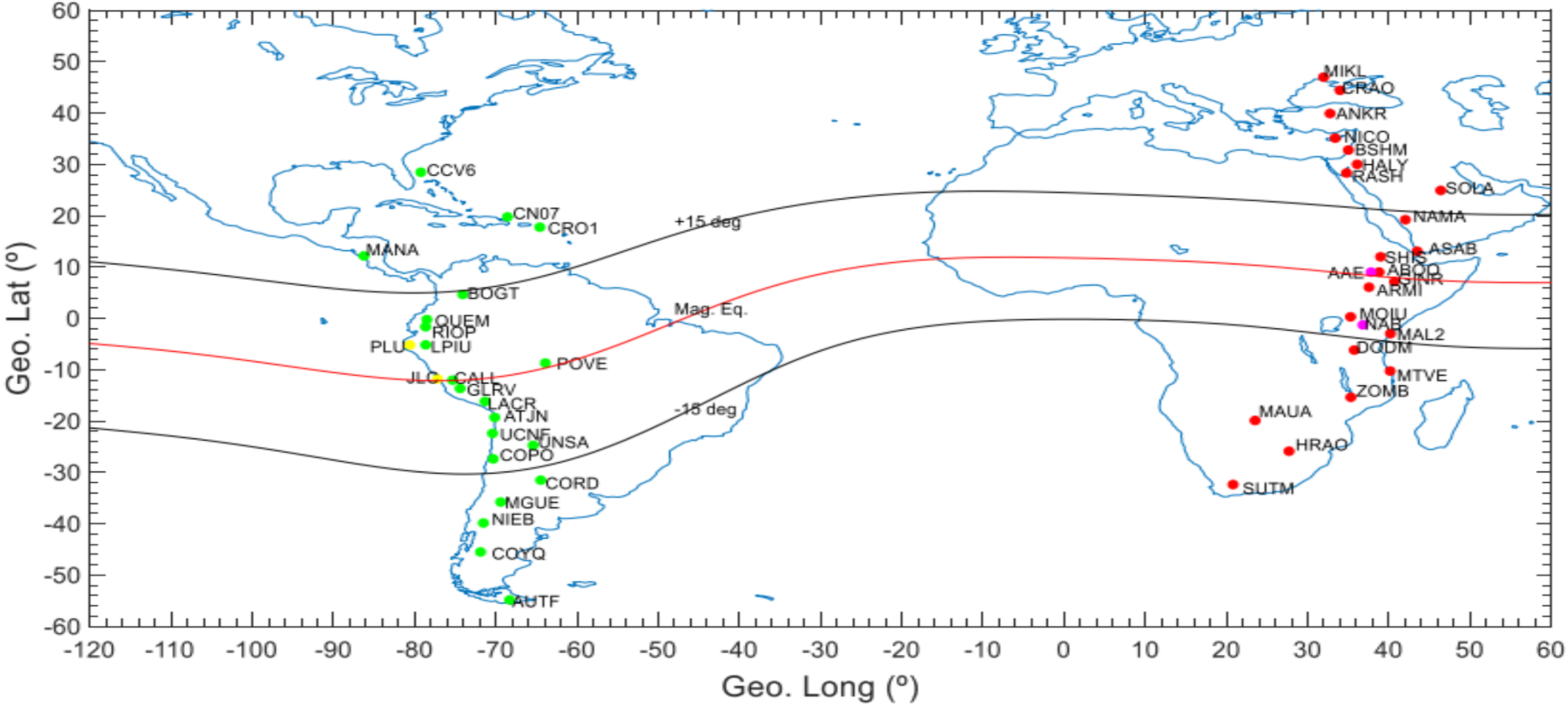

Figure 2: World map, indicating the locations of Global Positioning System (GPS) stations and the magnetometer stations in the American sector (green and yellow) and the Africa sector (red and magenta) for 2014 SSW events.

RESULTS AND DISCUSSION

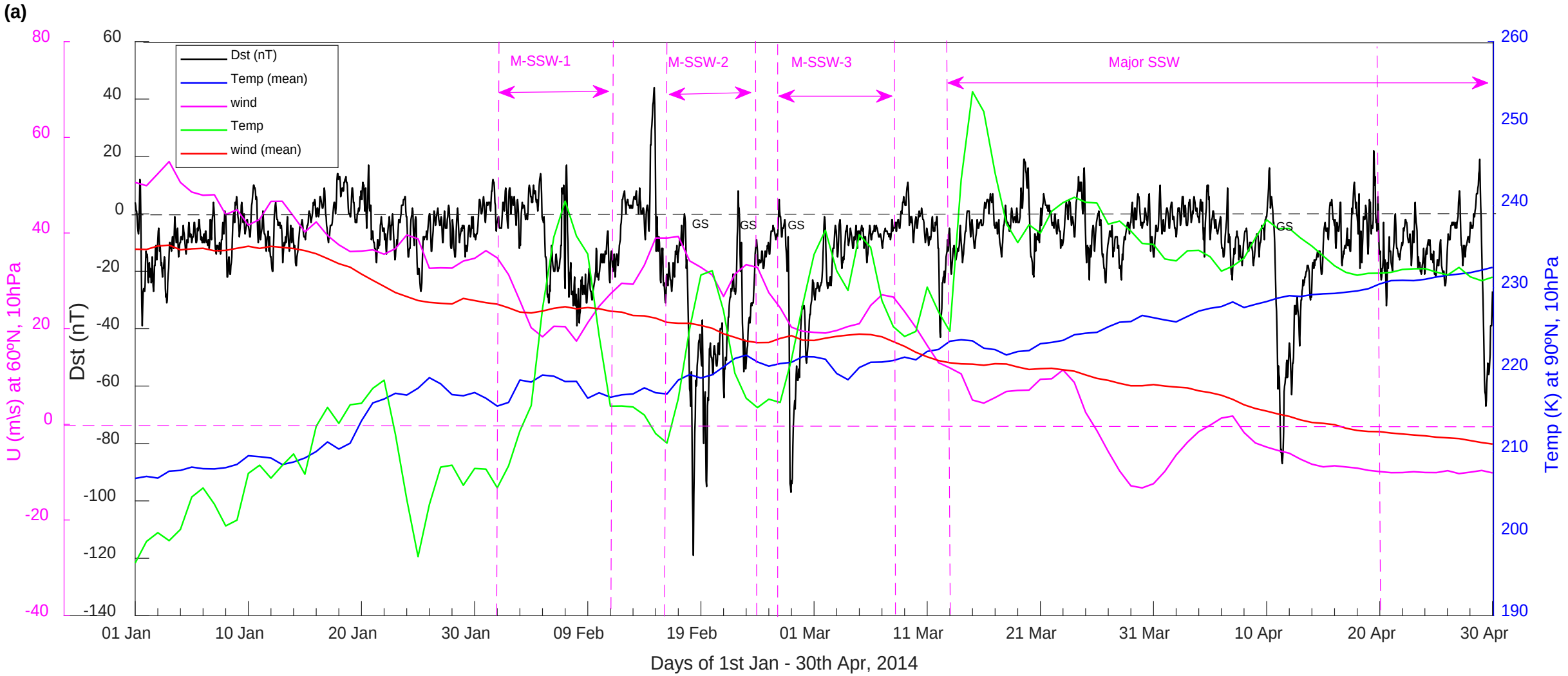

Figure 3: Stratospheric zonal mean air temperature at 90ºN, stratospheric historic zonal mean air temperature at 90ºN, stratospheric zonal mean zonal wind at 60ºN, stratospheric historic zonal mean zonal wind at 60ºN, all at 10 hPa, and daily variations of Dst index, all from 1st January–30th April 2014. M-SSW-1 represents the period of first minor SSW, M-SSW-2 for second minor SSW, M-SSW-3 for third minor SSW, and GS represents the periods of geomagnetic storms. The first GS is a dual-peak storm

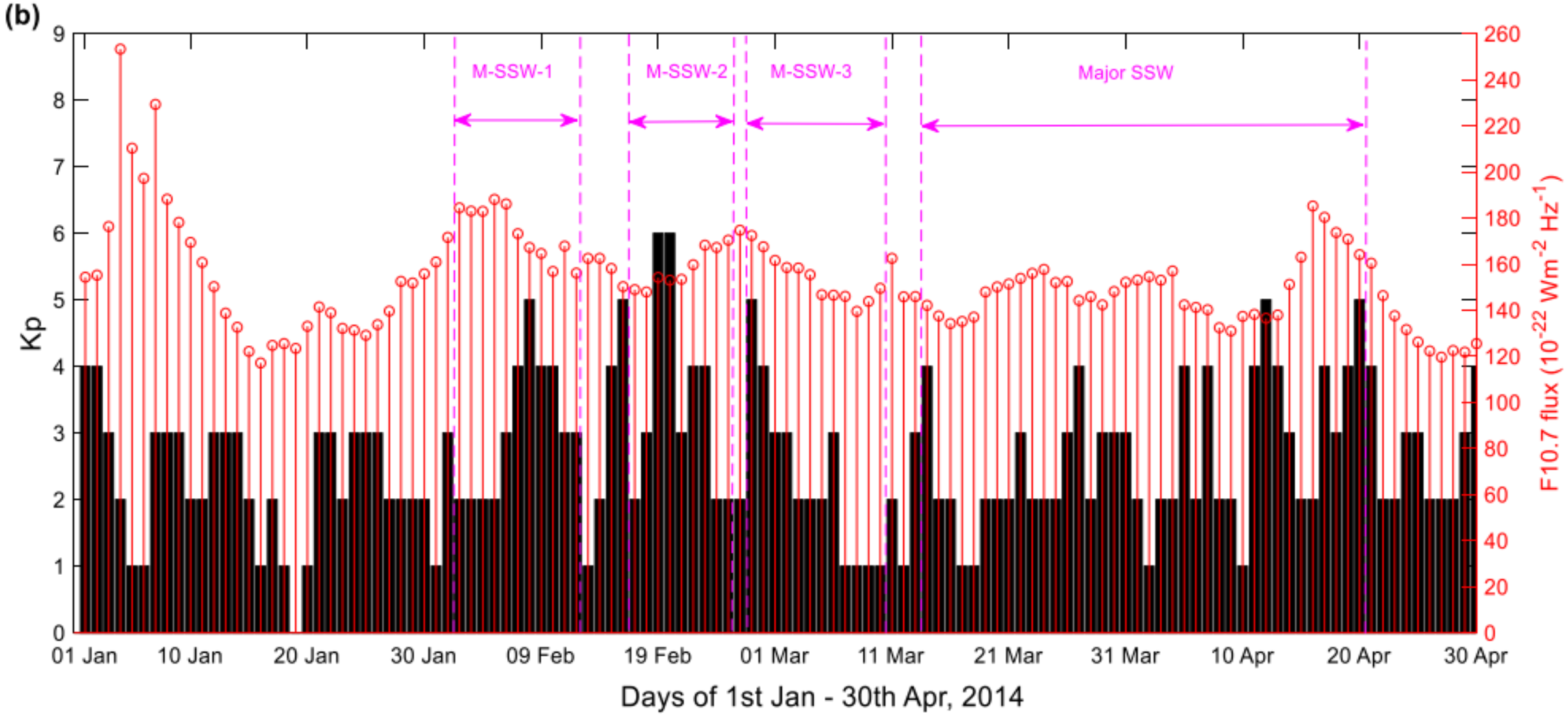

Figure 4: Kp index and F10.7cm solar flux from January 1 to April 30, 2014.

Table 1: Properties of the Sudden stratospheric Warming (SSW) Events that occurred during the 2014 period

Duration of the 2014 SSW Events	**SSW Designation**	**SSW Classification**	**Date of SSW Peak Temperature**	**Temperature Peak (K)**
2nd -12th Feb	M-SSW-1	Minor	8th Feb, 2014	240
17 – 25th FEB	M-SSW-2	Minor	21st Feb, 2014	232
27th FEB – 10th Mar	M-SSW-3	Minor	3rd and 6th Mar, 2014	237 and 237
14th – 20th Apr	Major	Major	16th Mar, 2014	253
Wind Reversal				Speed (m/s)
25th Mar, 2014				17 m/s

Table 2: Properties of geomagnetic storm that occurred during the 2014 SSW period

Date of Storm	Minimum Dst (nT)	Storm Classification	Time of storm onset/ Minimum Dst (UT)	African Sector (LT)	American Sector (LT)
19-02-2014	-119	Major	13:30/09:00	16:39/12:00	08:30/04:00
20-02-2014	-95	Moderate	NA/13:00	NA/16:00	NA/08:00 D
23-02-2014	-55	Moderate	07:30/19:00	10:30/22:00	02:30/14:00
27-02-2014	-97	Moderate	10:25/00:00	13:25/03:00	05:25/19:00
12-04-2014	-87	Moderate	05:52/09:00	10:52/12:00	00:52/04:00

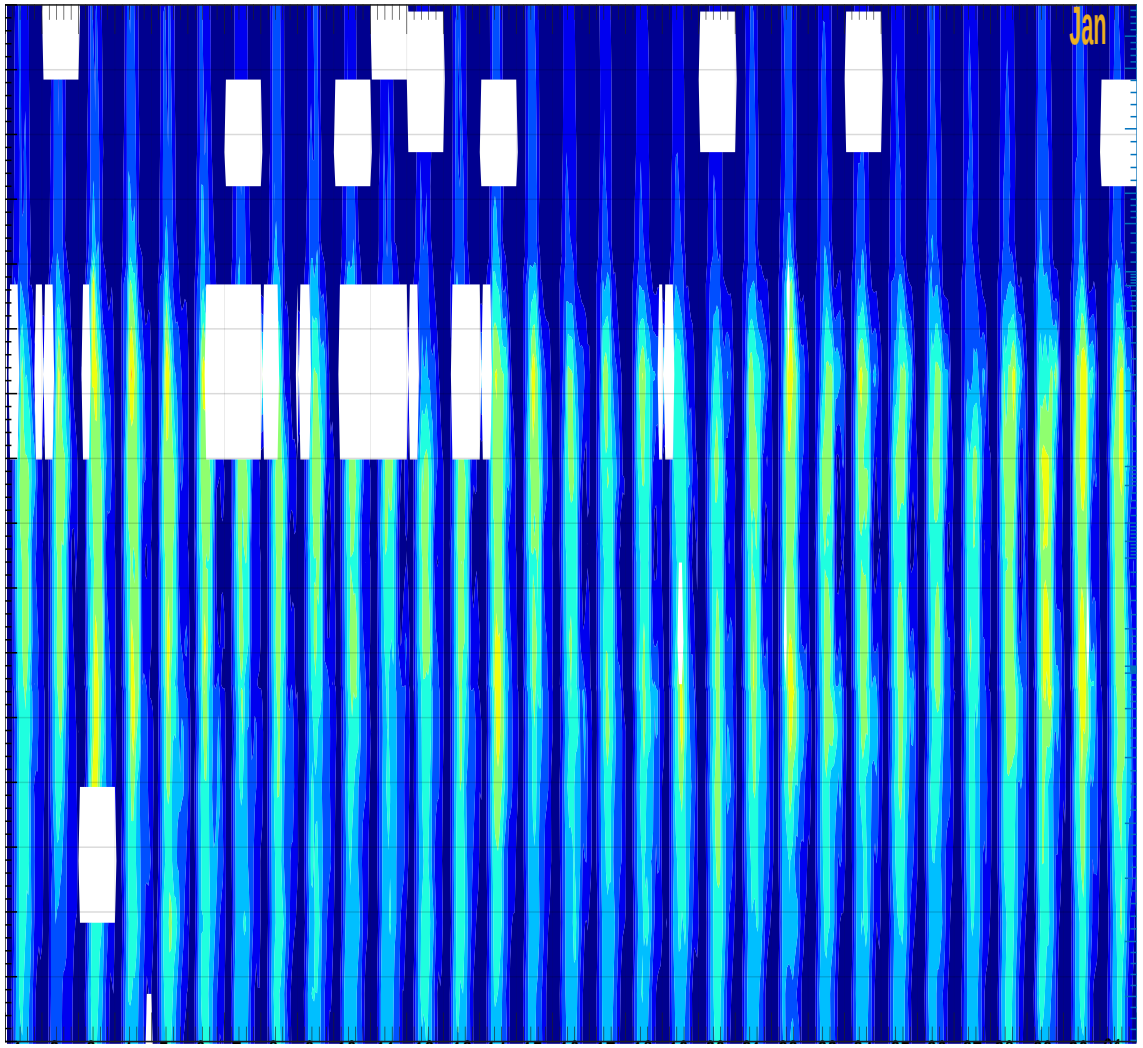

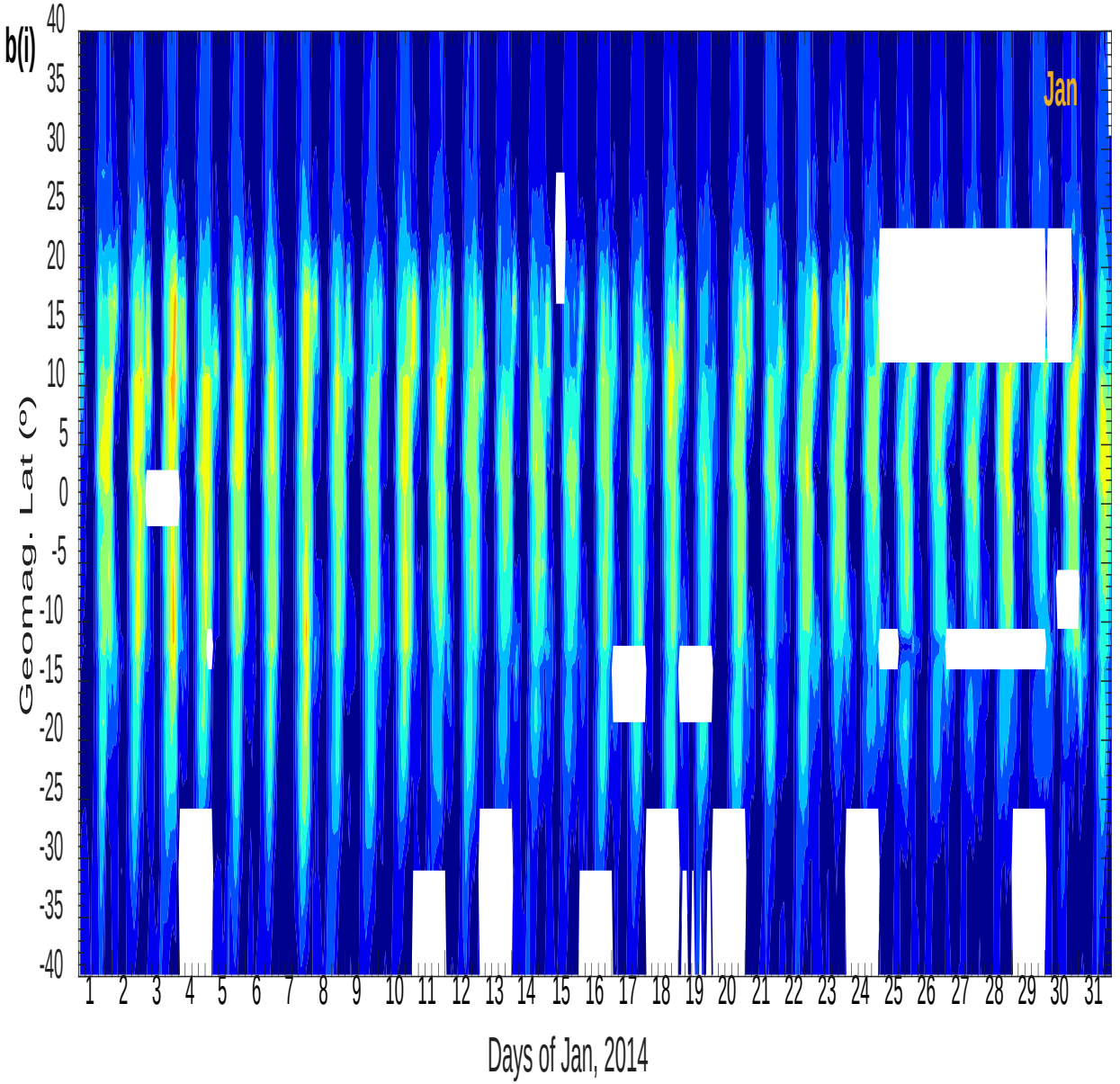

Figure 5: Day-to-day variations of EIA (TEC) from 1st January–30th April, 2014 (a) African sector: a(i) representing January (b) American sector: b(i) representing January.

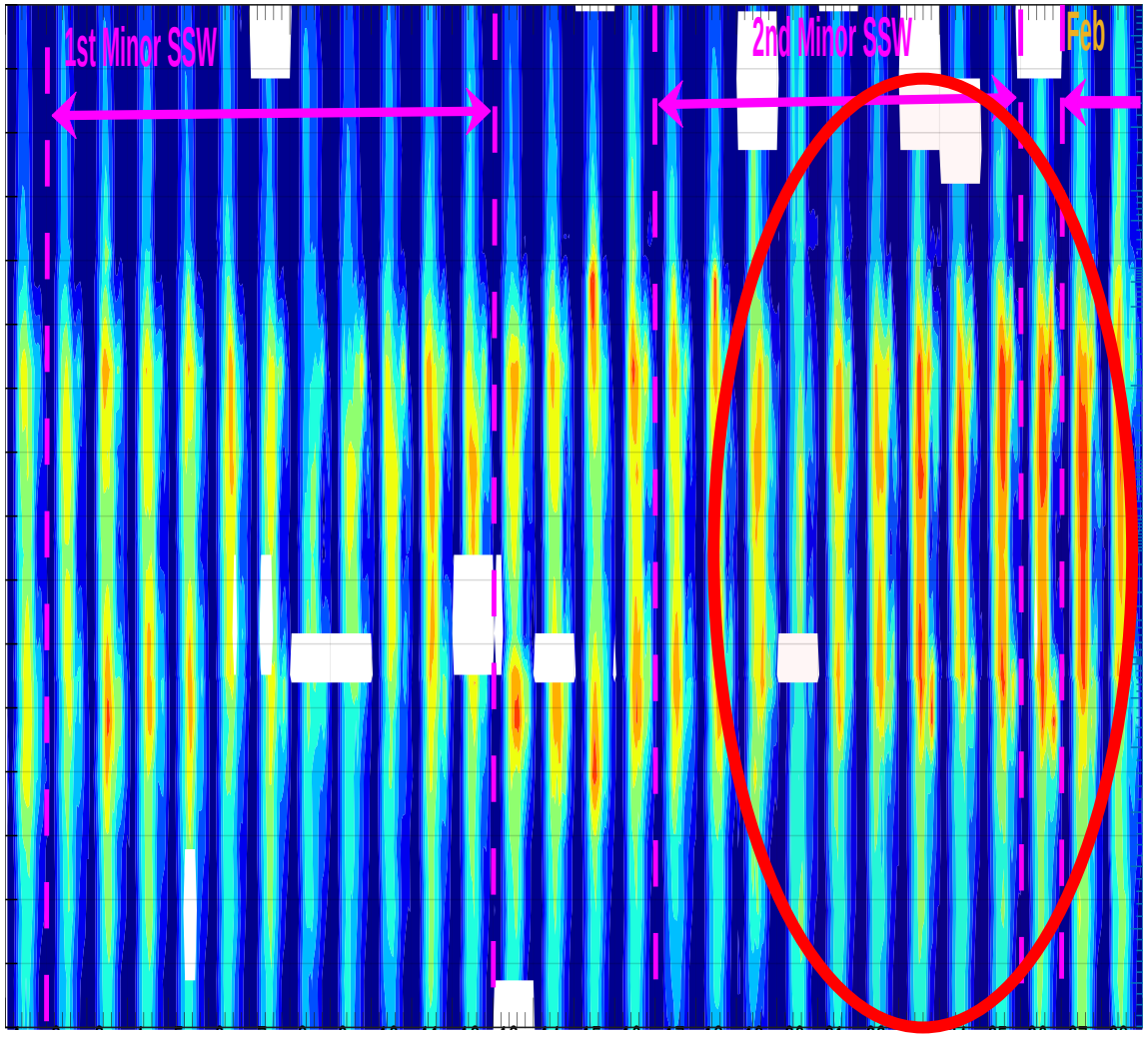

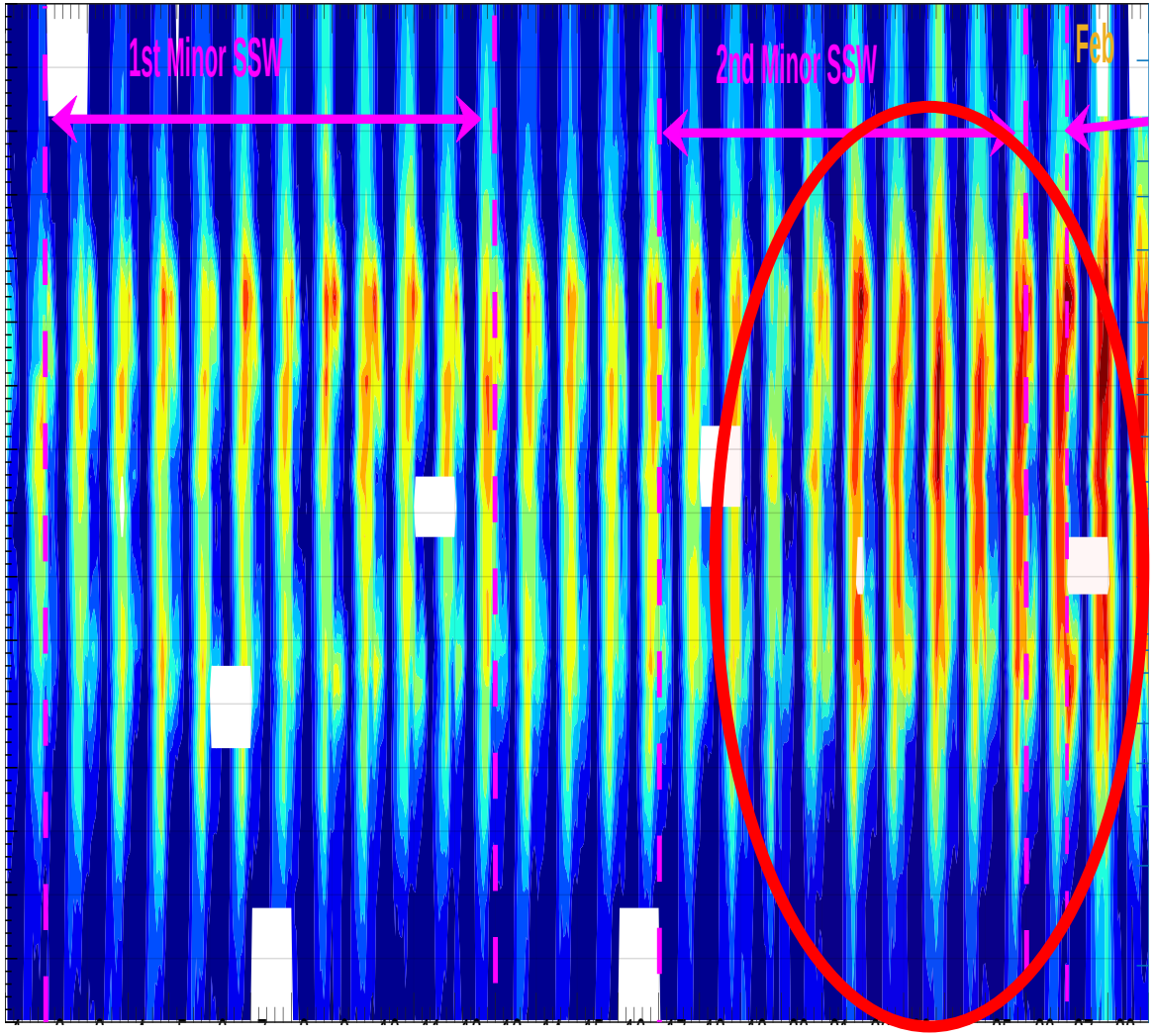

Figure 5: Day-to-day variations of EIA (TEC) from 1st January–30th April, 2014 (a) African sector: a(ii) representing February (b) American sector: b(ii) representing February.

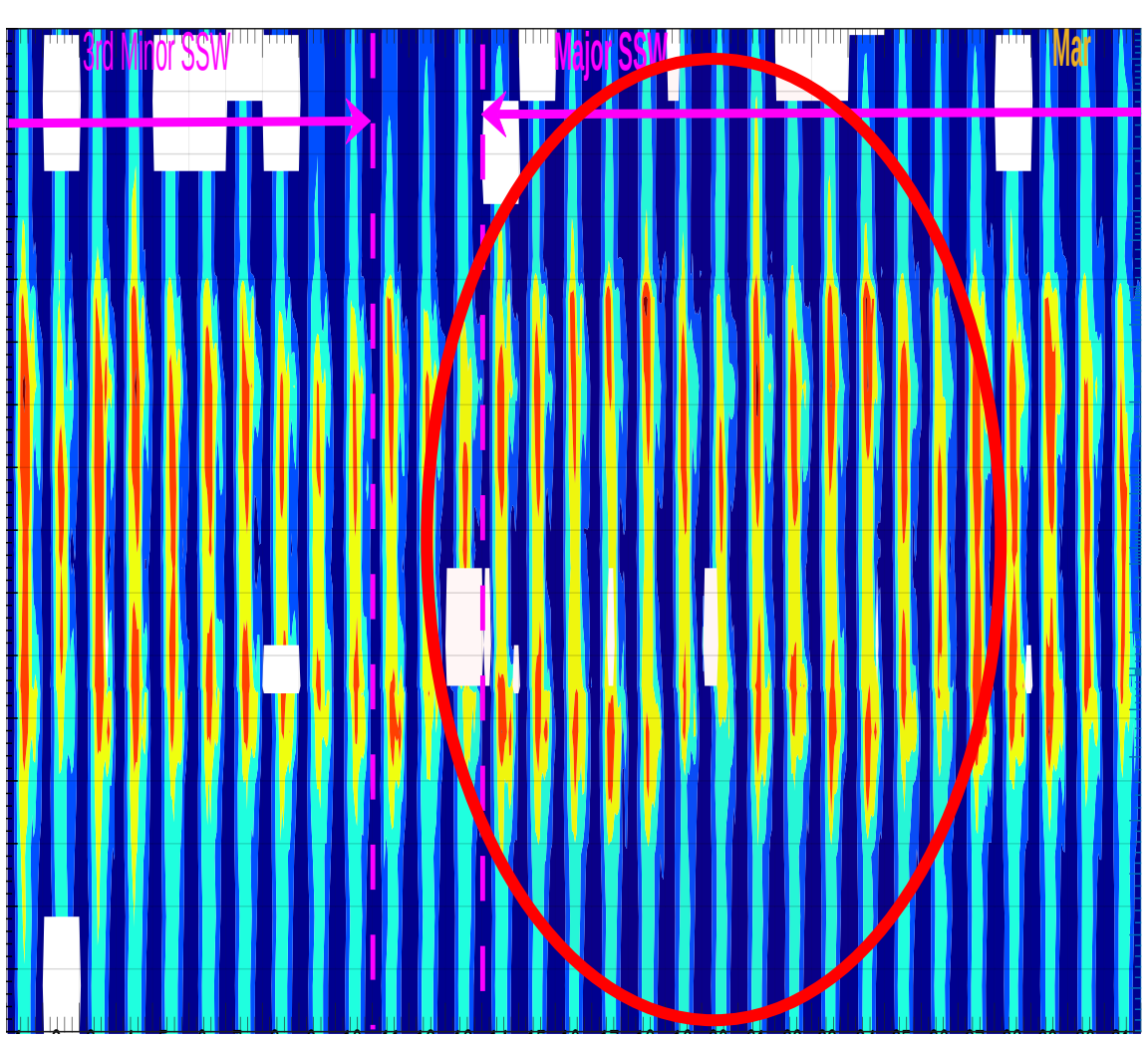

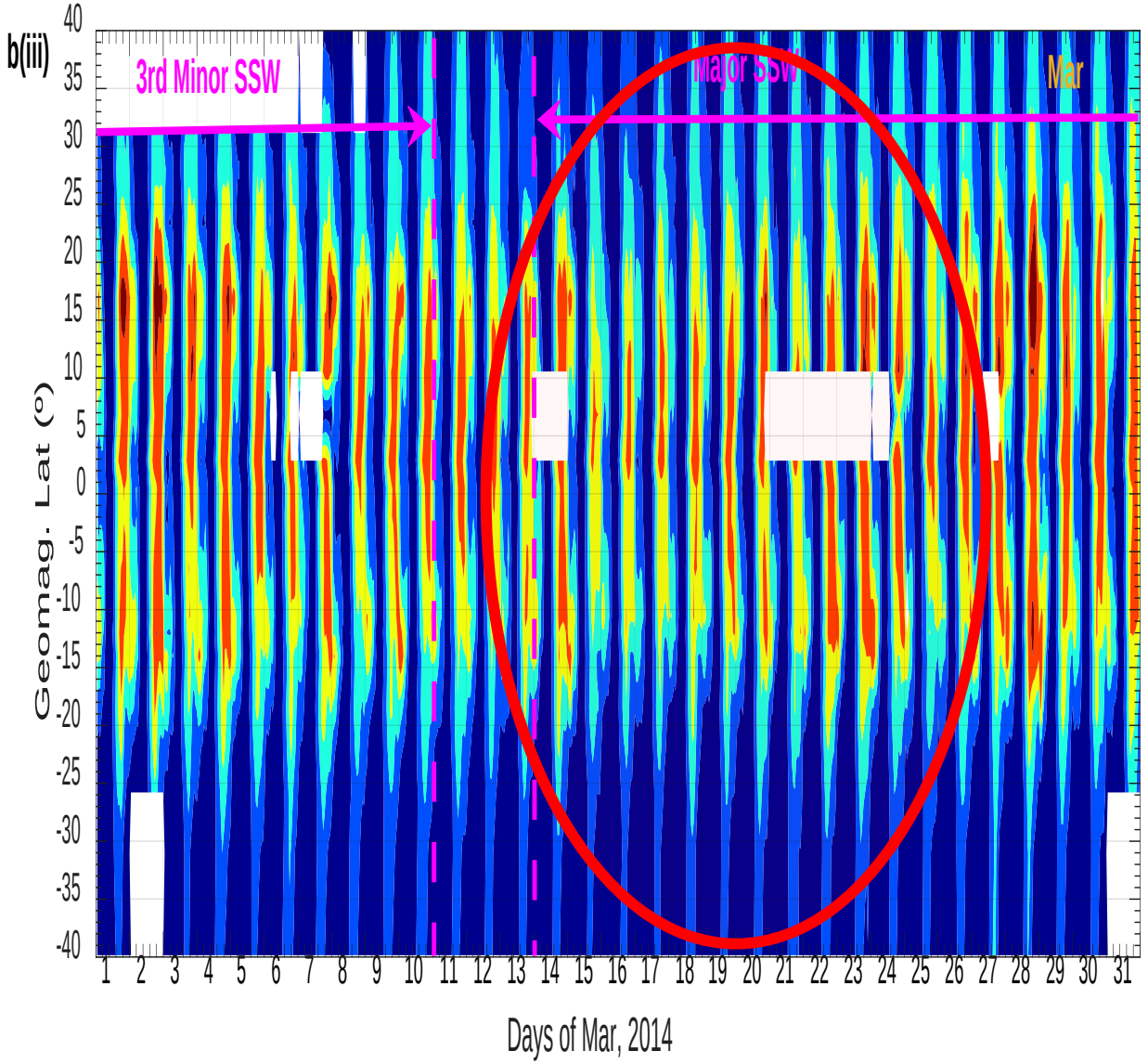

Figure 5: Day-to-day variations of EIA (TEC) from 1st January–30th April, 2014 (a) African sector: a(iii) representing March (b) American sector: b(iii) representing March.

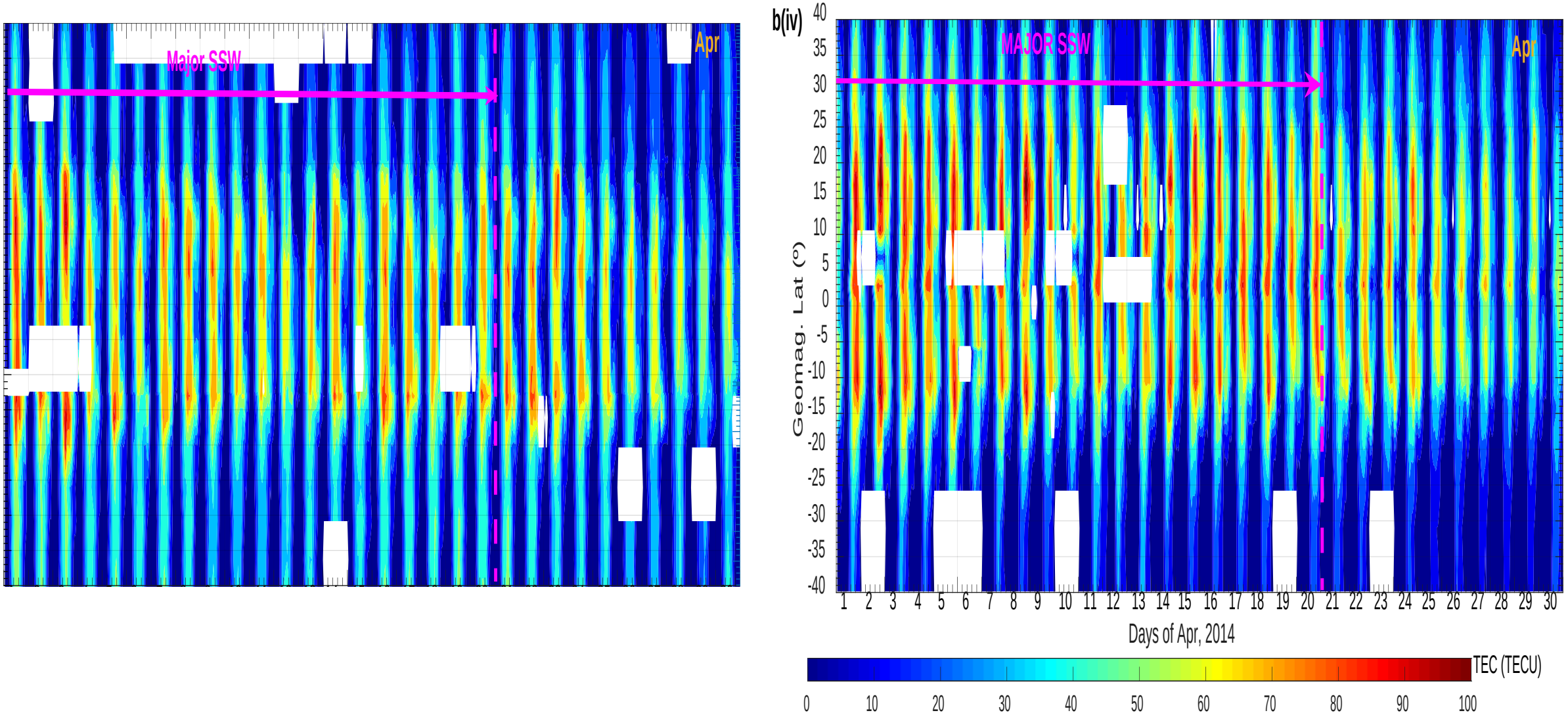

Figure 5: Day-to-day variations of EIA (TEC) from 1st January–30th April, 2014 (a) African sector: a(iv) April (b) American sector: b(iv) April.

Table 3: EIA Crests locations in the African and American Sectors during 2014 SSW event

S/N	Events	Date	EIA Crests Location African Sector		EIA Crests Location American Sector	
			NH (°N)	SH (°S)	NH (°N)	SH (°S)
1.	Pre-SSW + extremely quiet geomagnetic activity days	16/1/14	8.2	14.0	10.2	11.0
2.		18/1/14	8.5	16.0	10.8	10.0
3.		19/1/14	8.5	16.8	5.0	10.0
4.		31/1/14	8.0	16.5	6.0	6.2
1.	SSW	8/2/14	4.2	10.0	15.4	13.0
2.		21/2/14	9.0	13.0	15.8	13.0
3.		3/3/14	12.0	13.5	16.0	12.0
		6/3/14	11.5	13.0	15.2	11.0
4.		16/3/14	14.0	16.2	13.0	12.0
1.	4 most quiet geomagnetic days of February, 2014	13/2/14	11.8	17.0	16.0	12.4
2.		14/2/14	11.6	17.2	15.8	12.0
3.		25/2/14	10.3	13.8	17.8	12.2
4.		26/2/14	10.0	15.0	18.0	13.8
1.	4 most quiet geomagnetic days of April, 2014	2/4/14	9.0	13.0	18.0	17.0
2.		6/4/14	8.0	8.0	15.0	7.0
3.		10/4/14	5.0	10.0	11.0	5.0
4.		16/4/14	6.0	14.0	16.0	8.0
1.	Geomagnetic storms	19/2/14	7.2	13.2	15.2	10.0
2.		20/2/14	7.2	8.6	17.0	10.0
3.		23/2/14	10.0	10.5	12.5	11.0
4.		27/2/14	10.0	12.2	18.0	13.0
5.		12/4/14	5.0	7.0	13.0	6.5

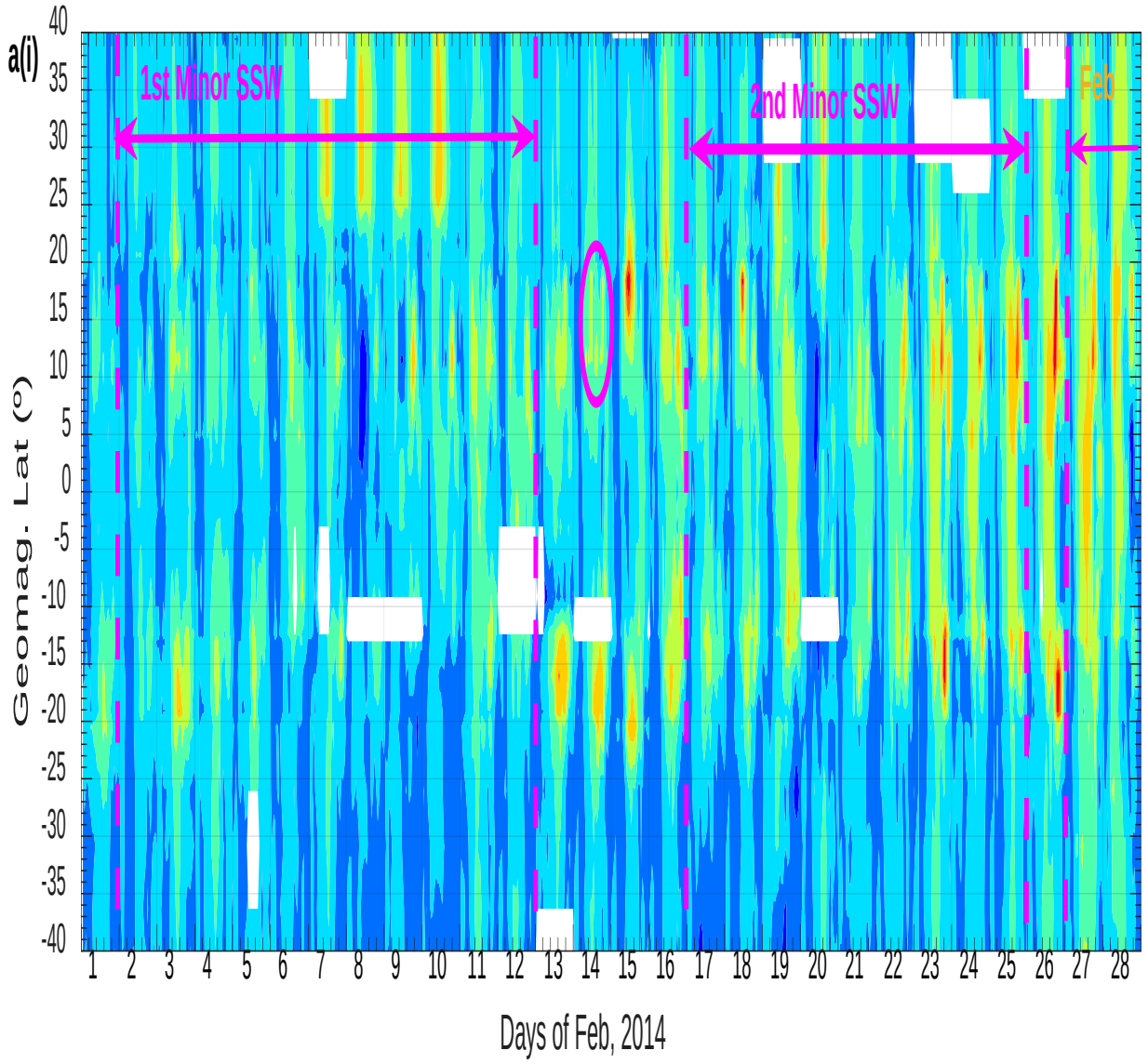

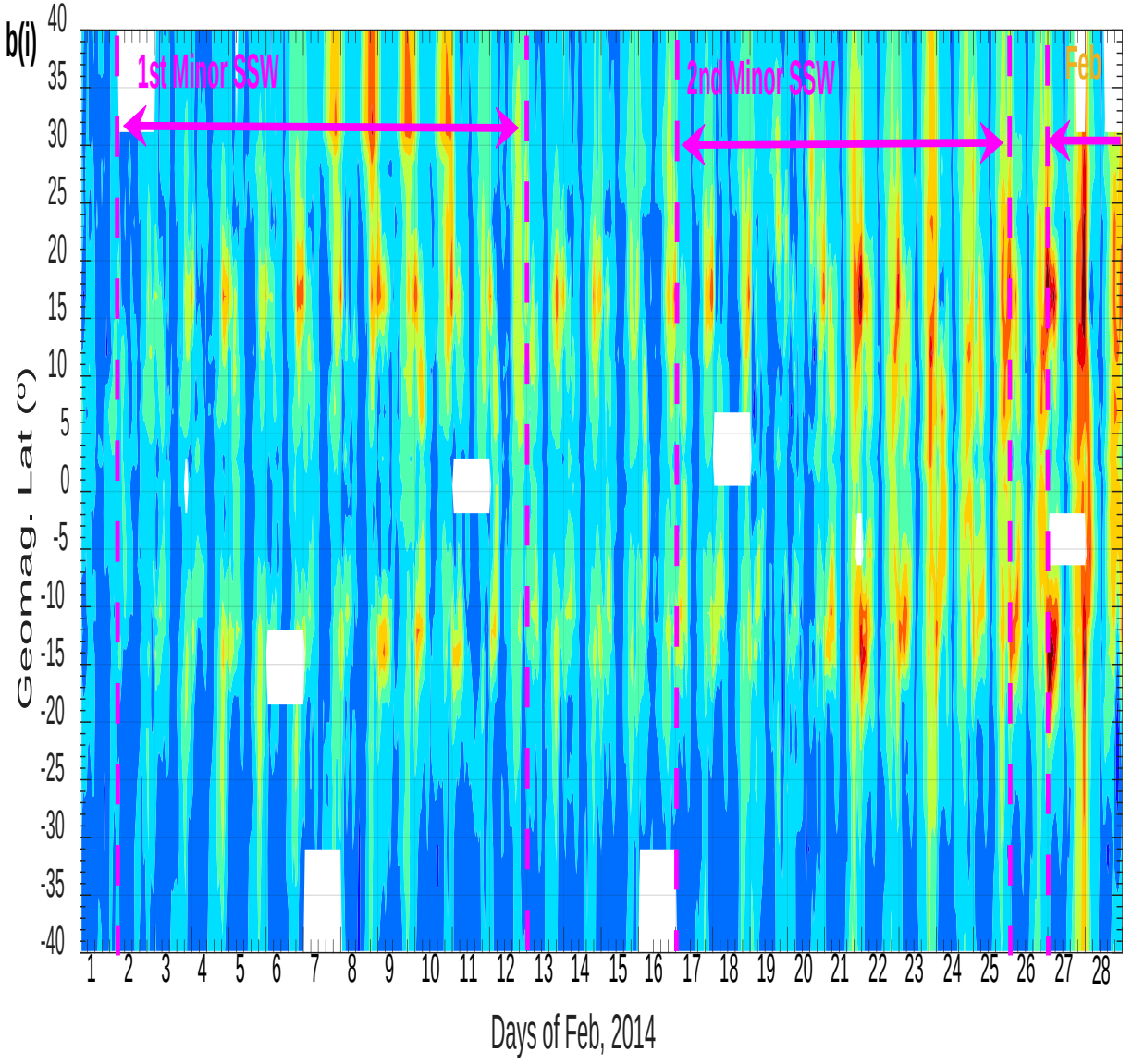

Figure 6: Day-to-day variations of EIA (ΔTEC) from 1st February–30th April, 2014 (a) African sector: a(i) representing February (b) American sector: b(i) representing February.

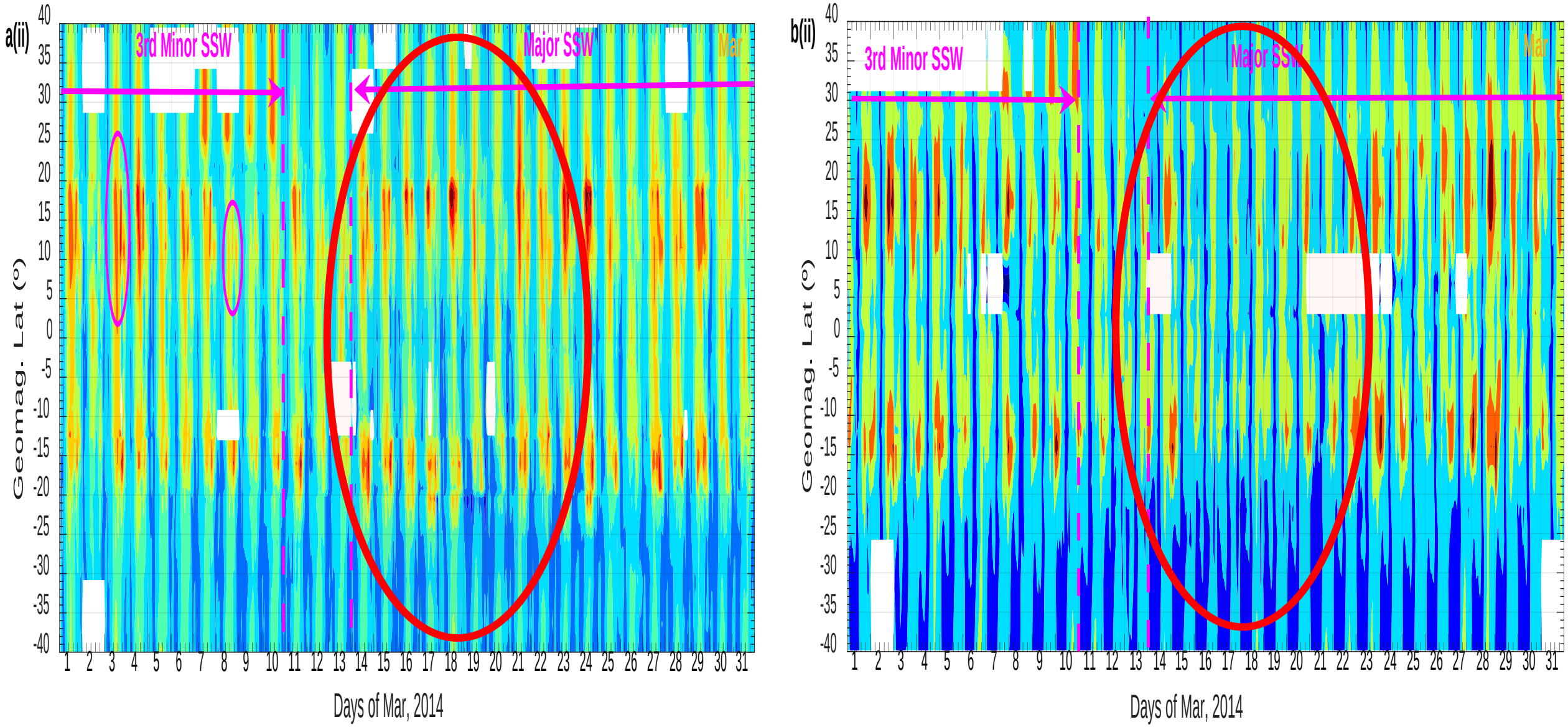

Figure 6: Day-to-day variations of EIA (ΔTEC) from 1st February–30th April, 2014 (a) African sector: a(ii) representing March (b) American sector: b(ii) representing March.

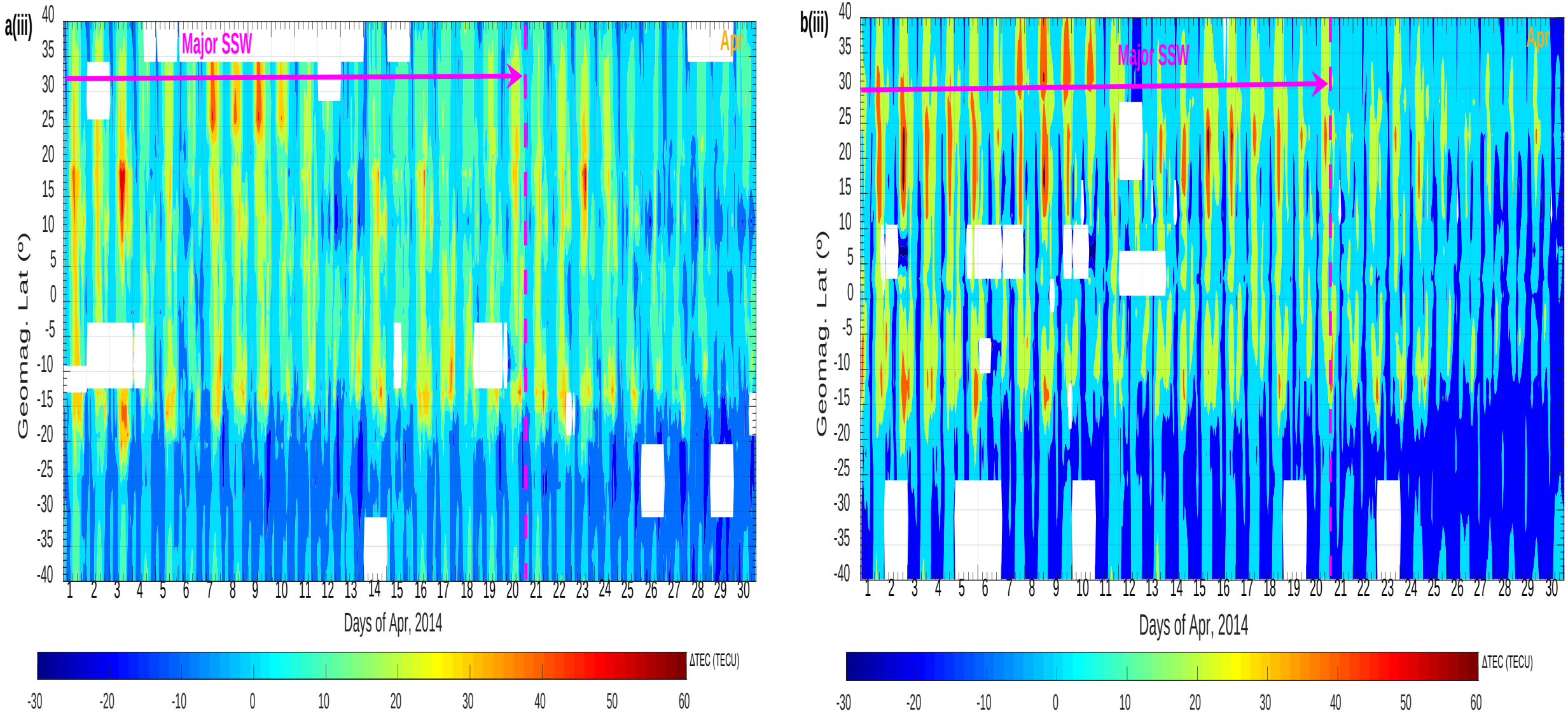

Figure 6: Day-to-day variations of EIA (ΔTEC) from 1st February–30th April, 2014 (a) African sector: a(iii) representing April (b) American sector: b(iii) representing April.

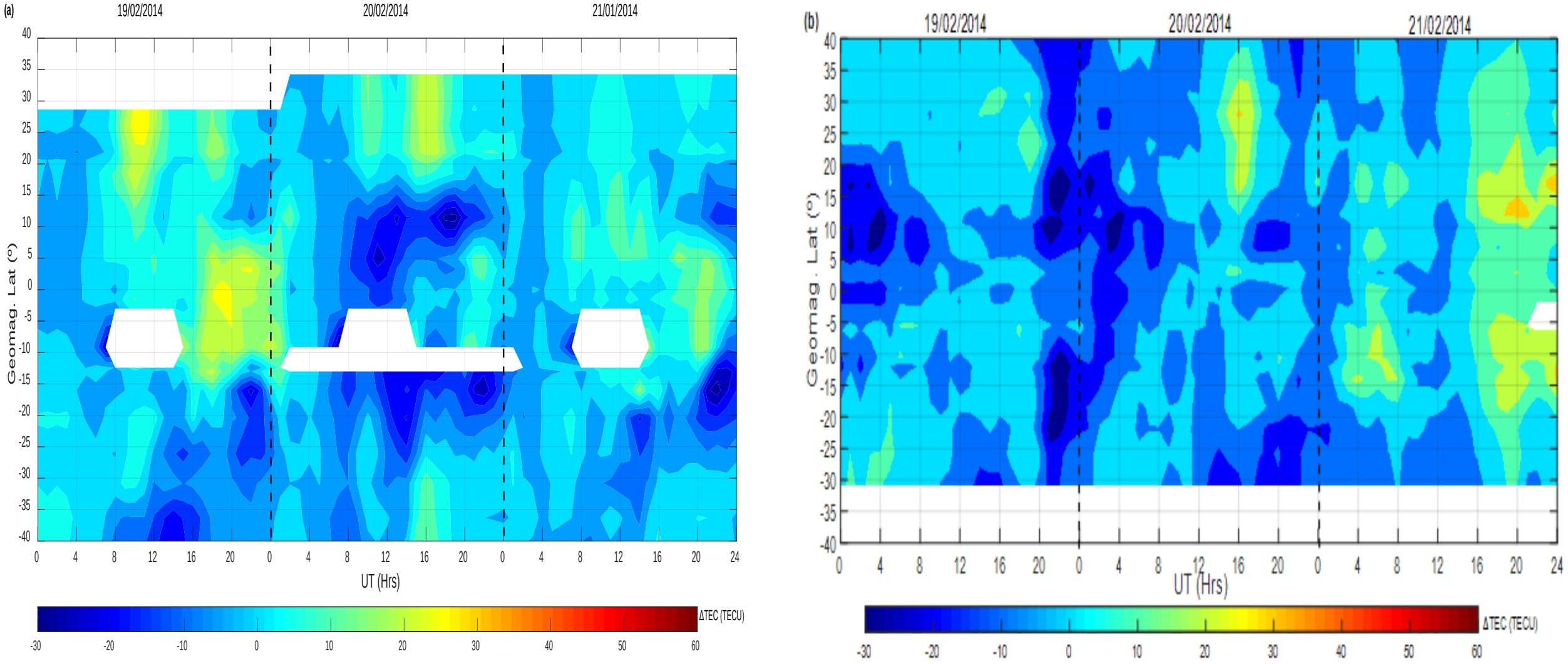

Figure 7: Removal of SSW-induced ionospheric effect from geomagnetic activity-induced ionospheric effect on 19–21st February, 2014 (19th (major geomagnetic storm), 20th (moderate geomagnetic storm), and 21st (recovery phase of the geomagnetic storm)). Ionospheric effect of 7th February, a day solely characterized with SSW event was used to filter the SSW.

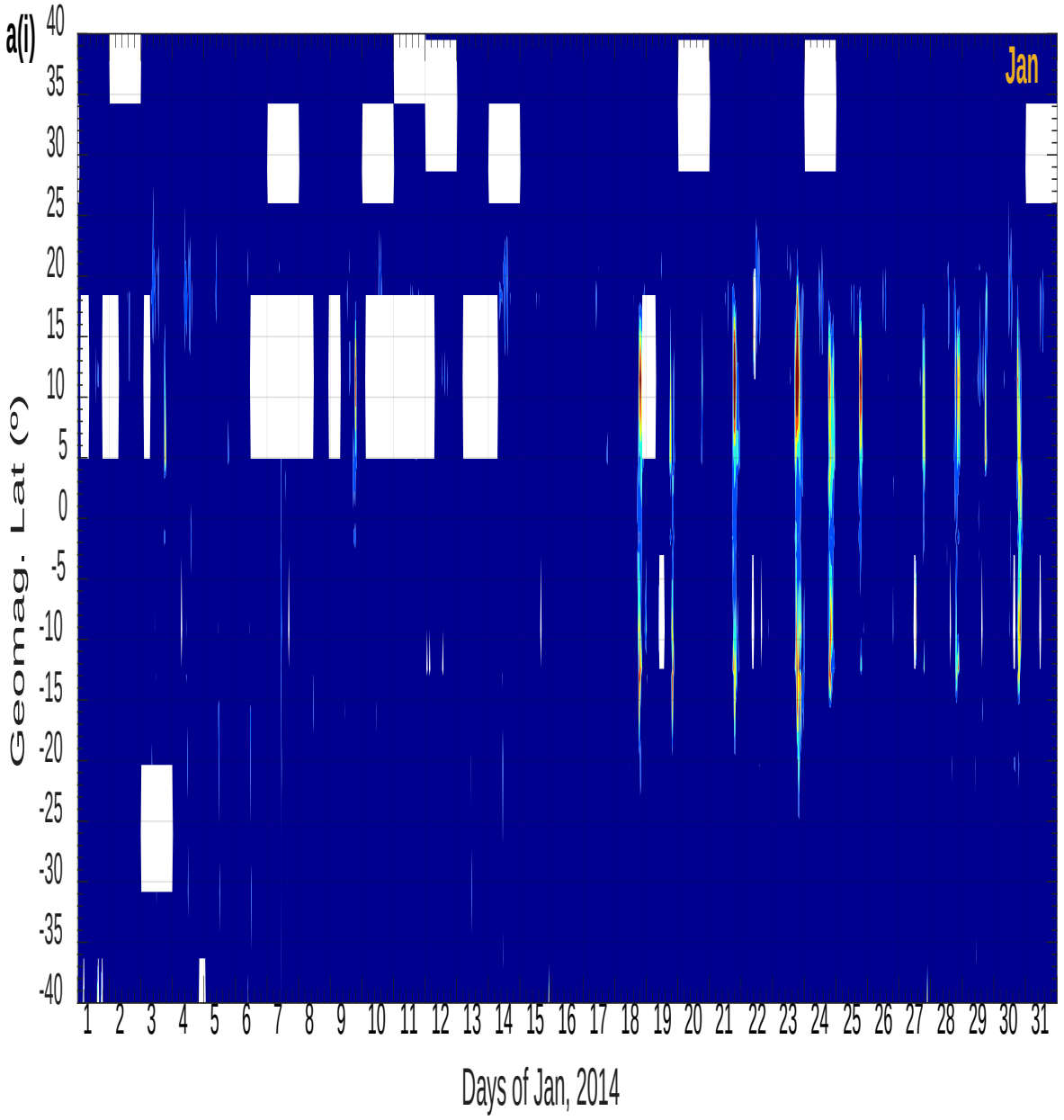

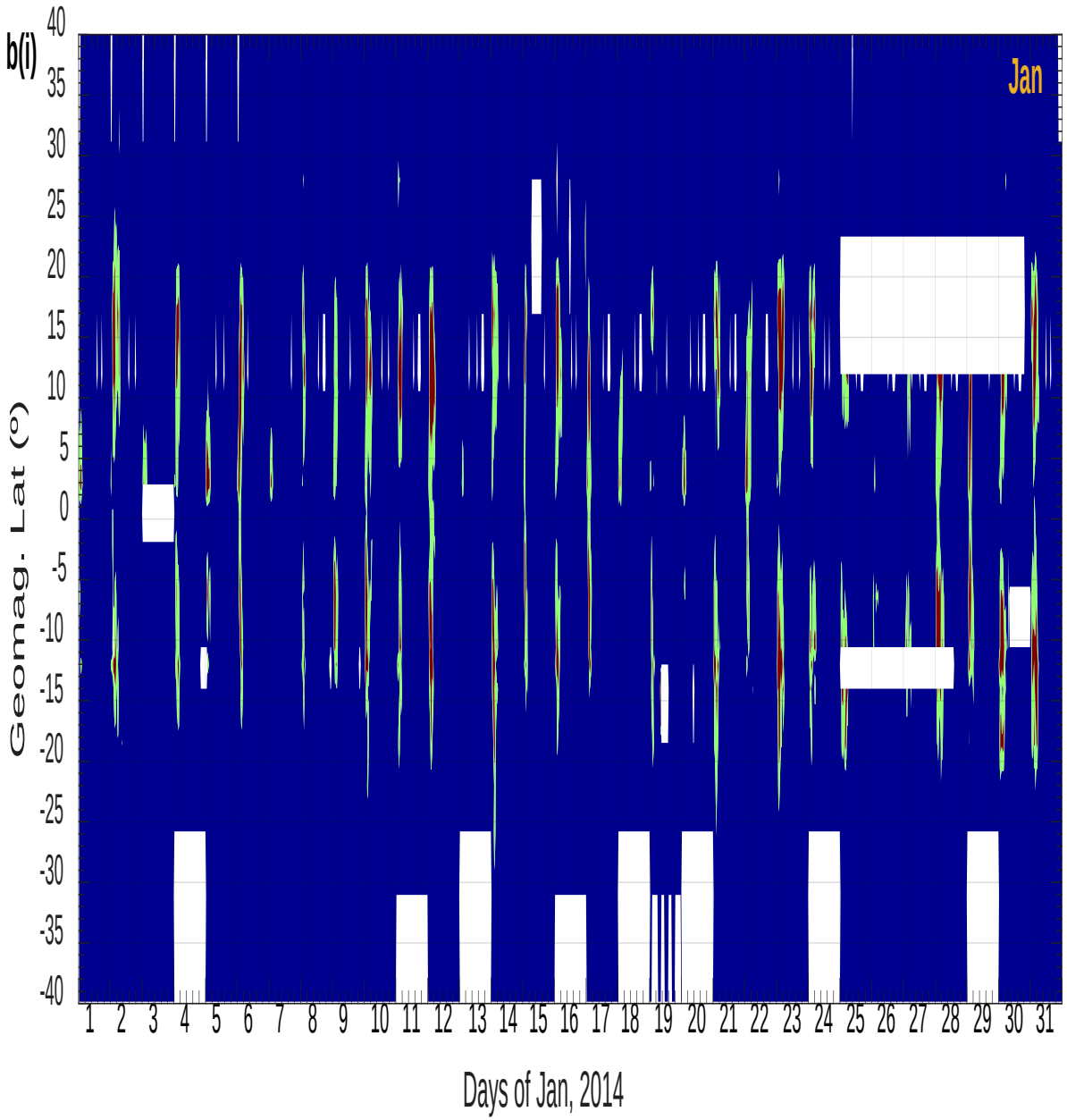

Figure 8: Day-to-day variations in ionospheric irregularities from 1st January–30th April, 2014 (a) African sector: a(i) representing January (b) American sector: b(i) representing January.

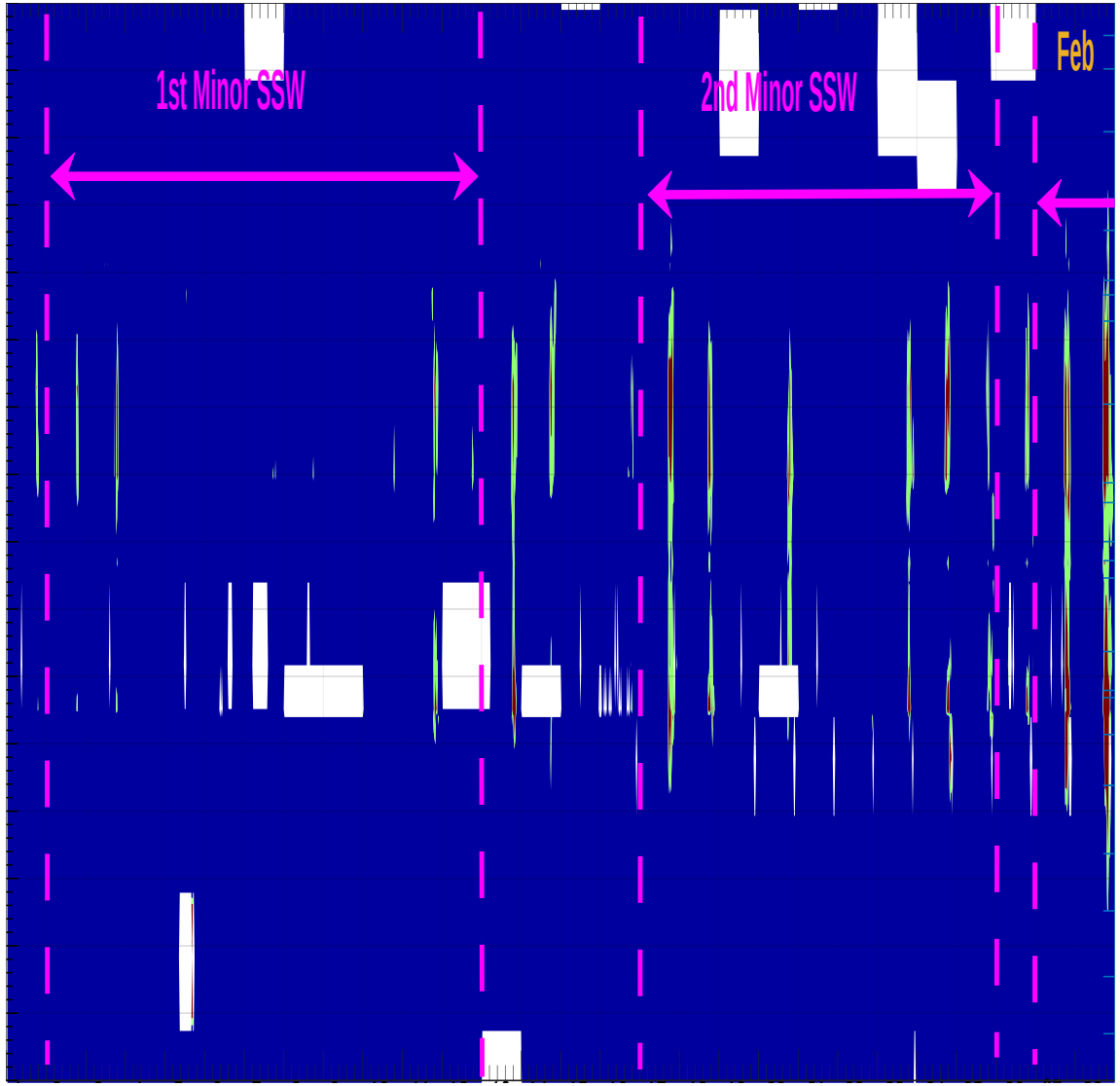

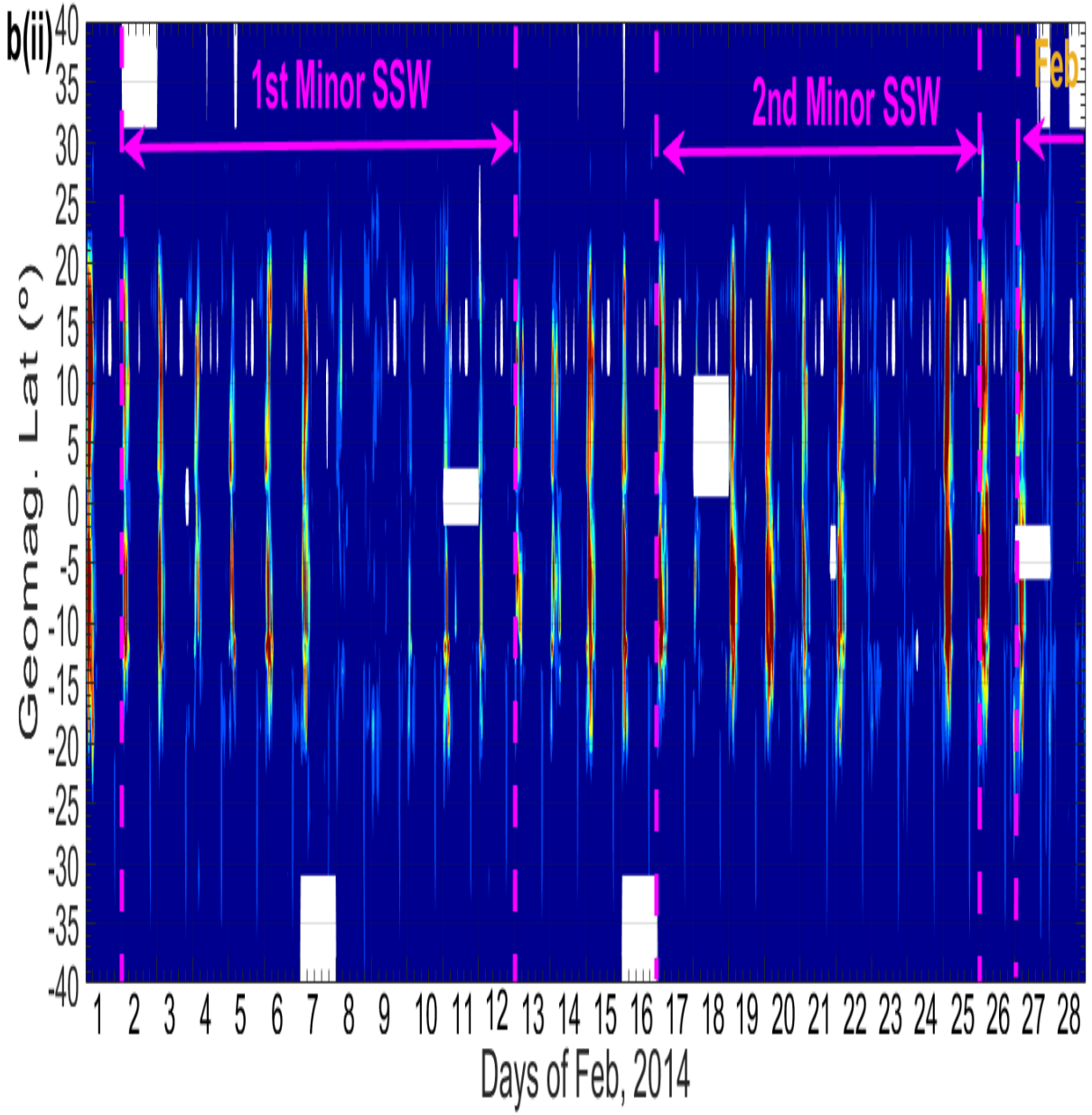

Figure 8: Day-to-day variations in ionospheric irregularities from 1st January–30th April, 2014 (a) African sector: a(ii) representing February (b) American sector: b(ii) representing February.

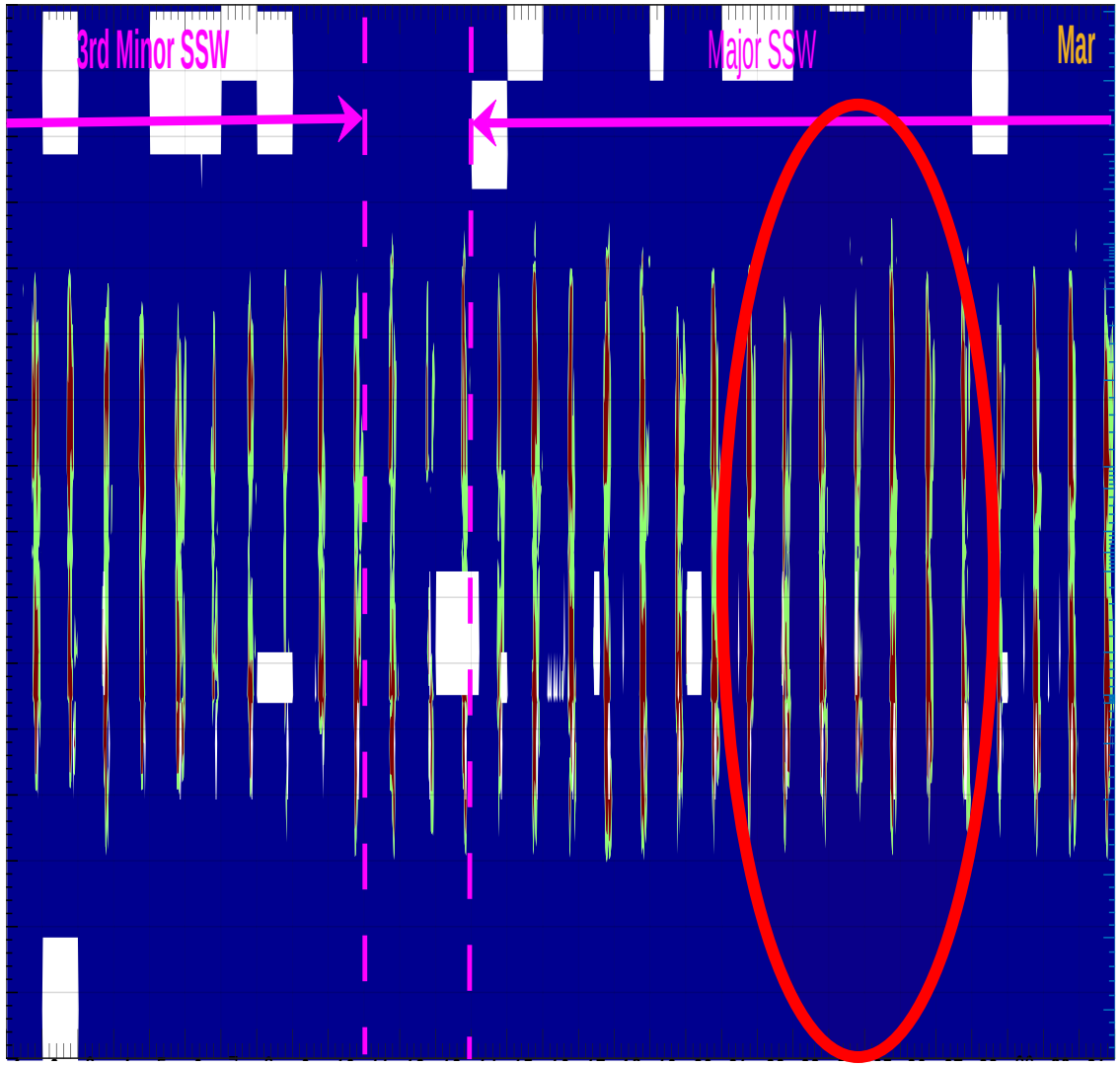

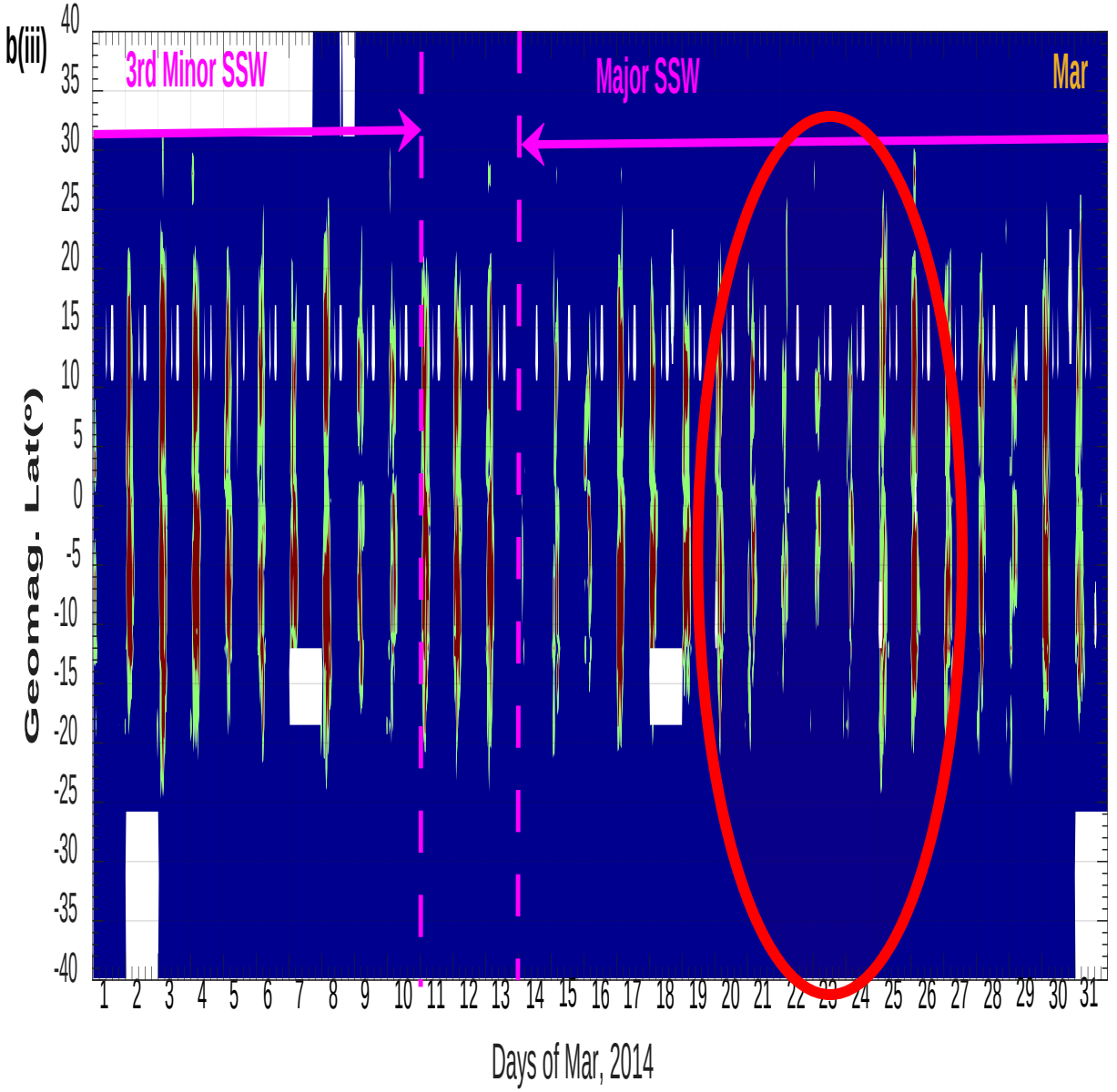

Figure 8: Day-to-day variations in ionospheric irregularities from 1st January–30th April, 2014 (a) African sector: a(iii) representing March (b) American sector: b(iii) representing March.

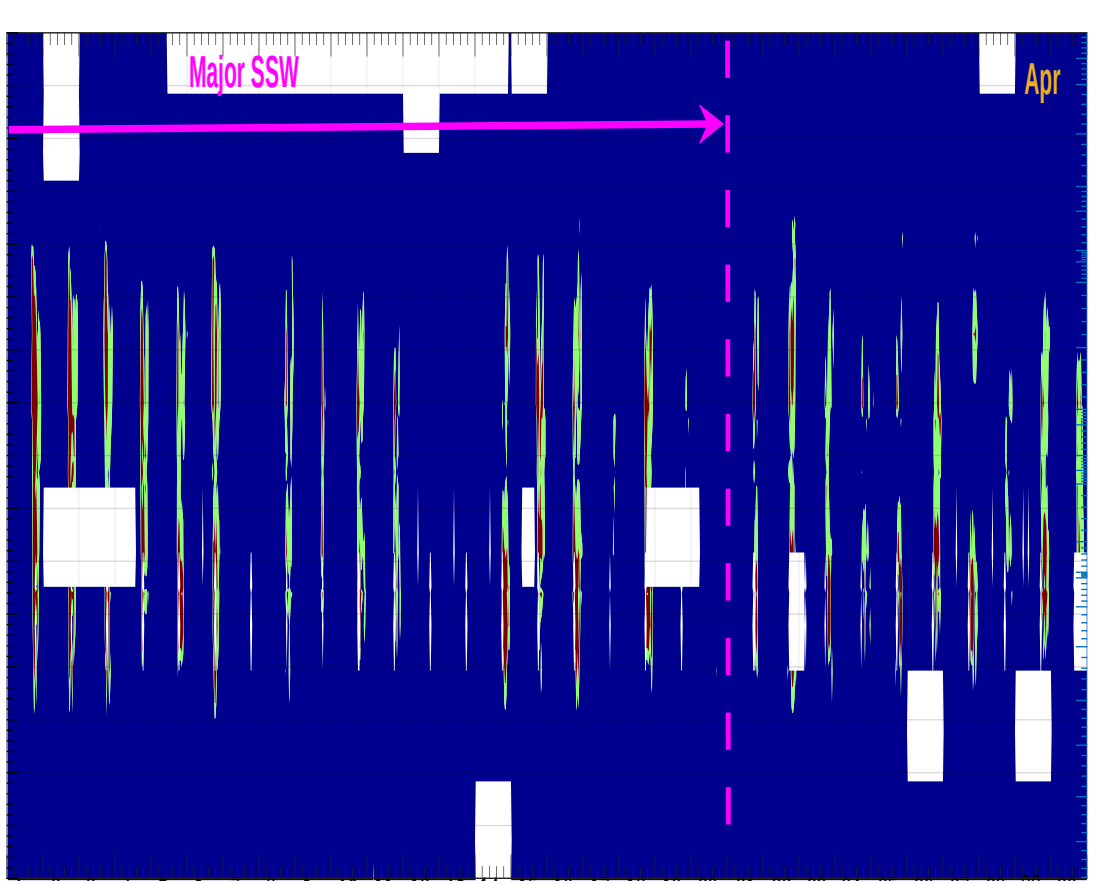

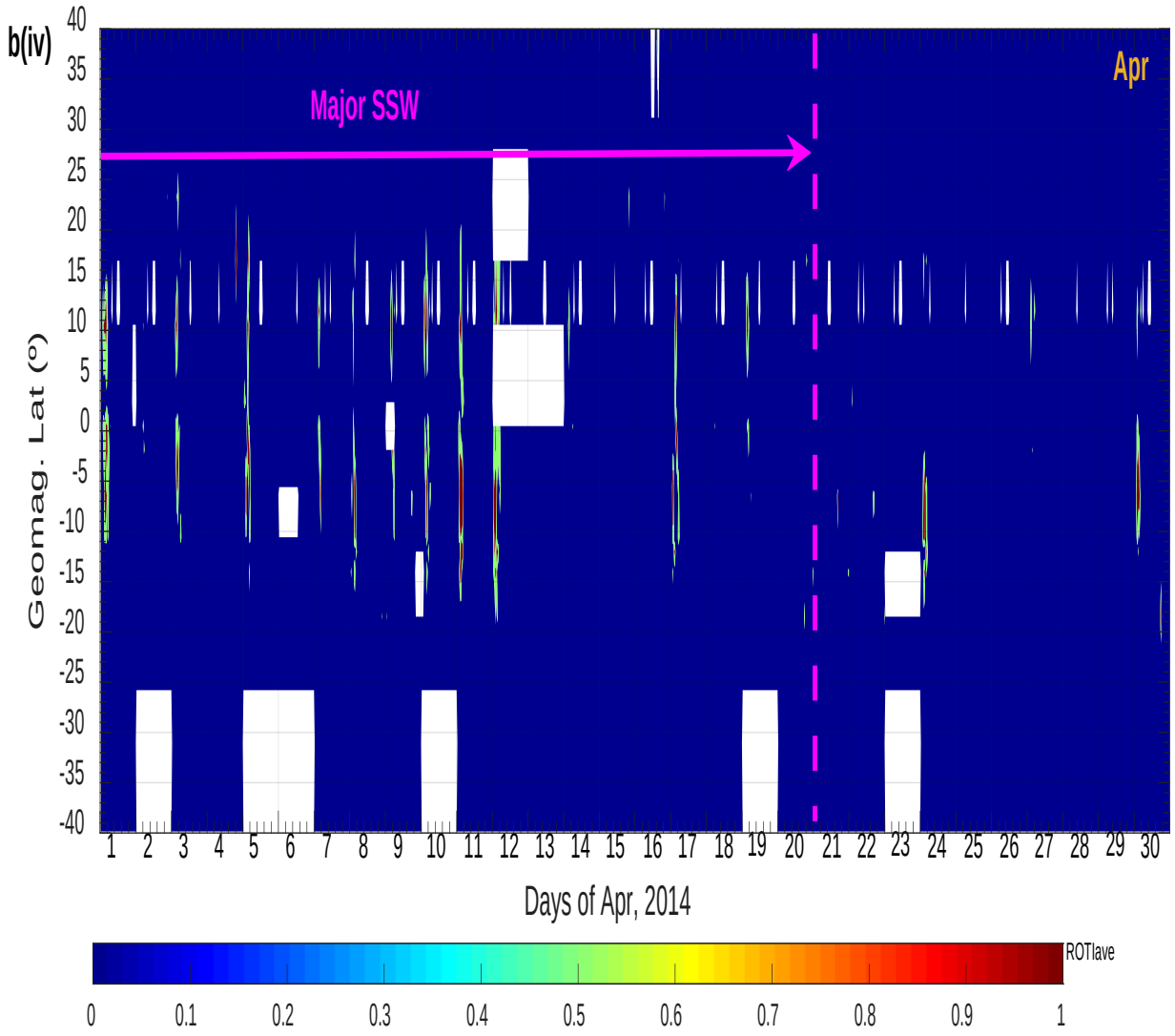

Figure 8: Day-to-day variations in ionospheric irregularities from 1st January–30th April, 2014 (a) African sector: a(iv) representing April (b) American sector: b(iv) representing April.

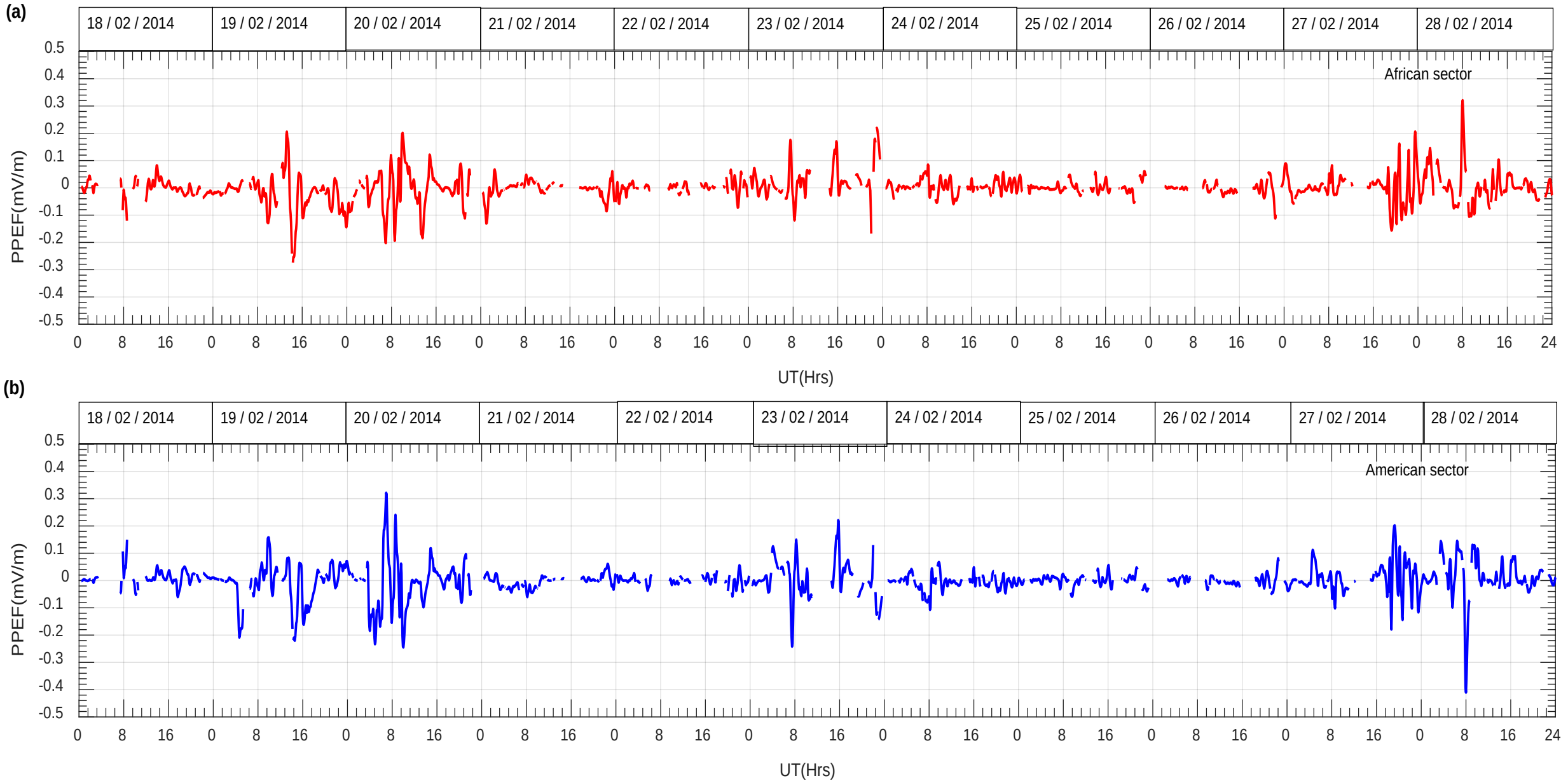

Figure 9: Day-to-day variations in Prompt Penetration Electric Field (PPEF)

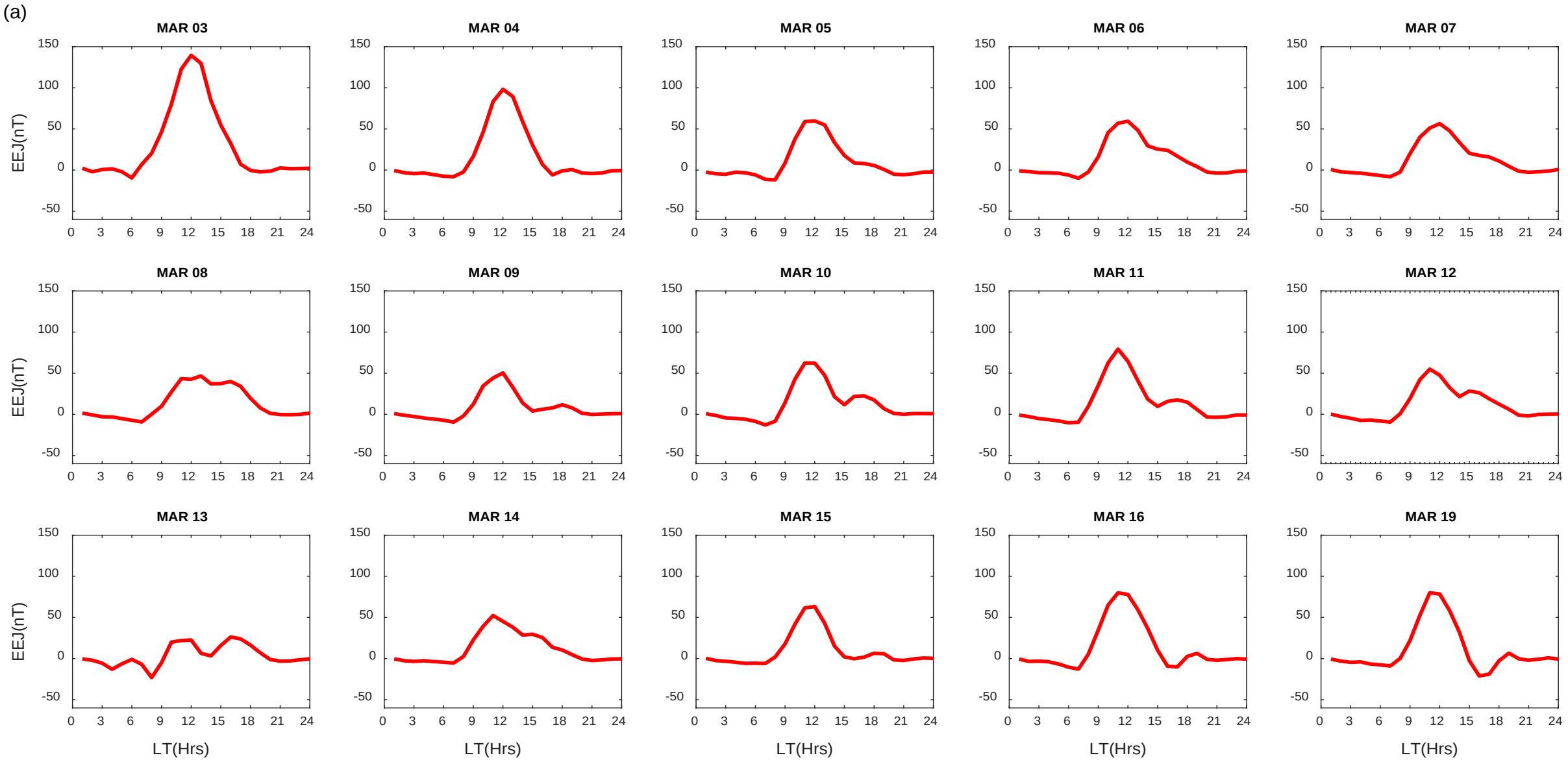

Figure 10: Equatorial electrojet current variation from 3–19th March, 2014: (a) African sector.

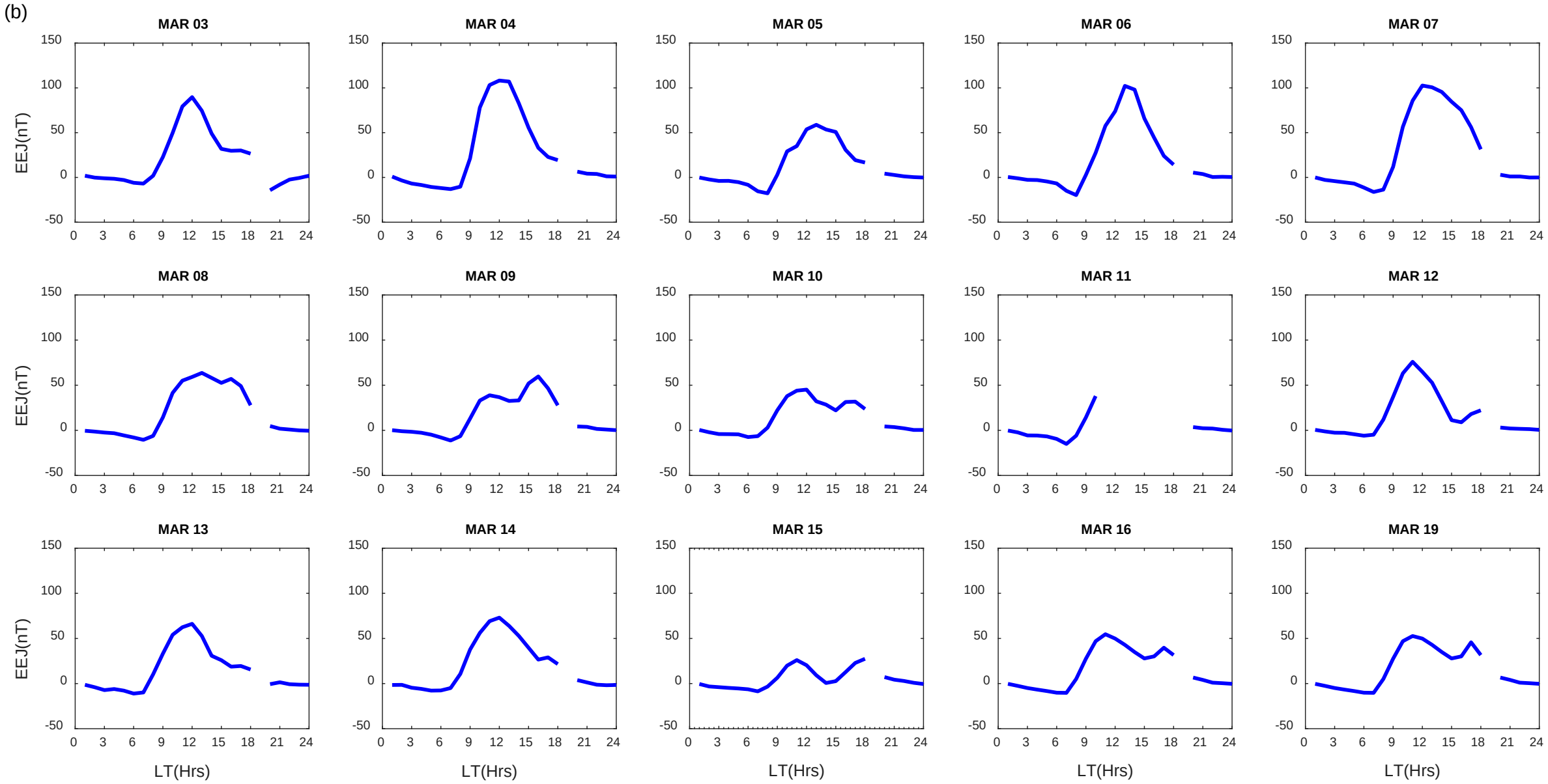

Figure 10: Equatorial electrojet current variation from 3–19th March, 2014: (b) American sector.

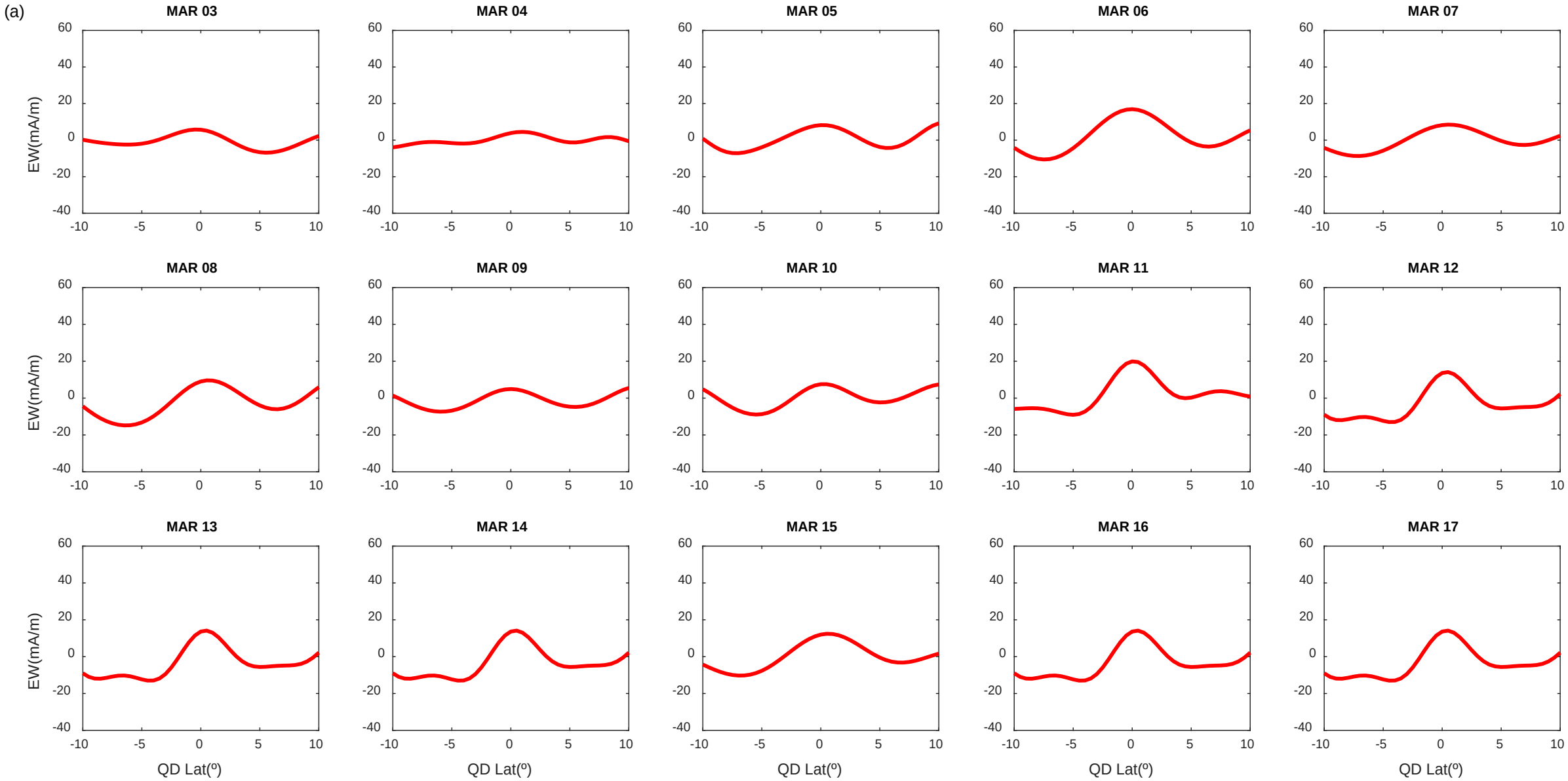

Figure 11: Day-to-day variations in eastward (EW) current density profile from 3–17th March, 2014: (a) African sector

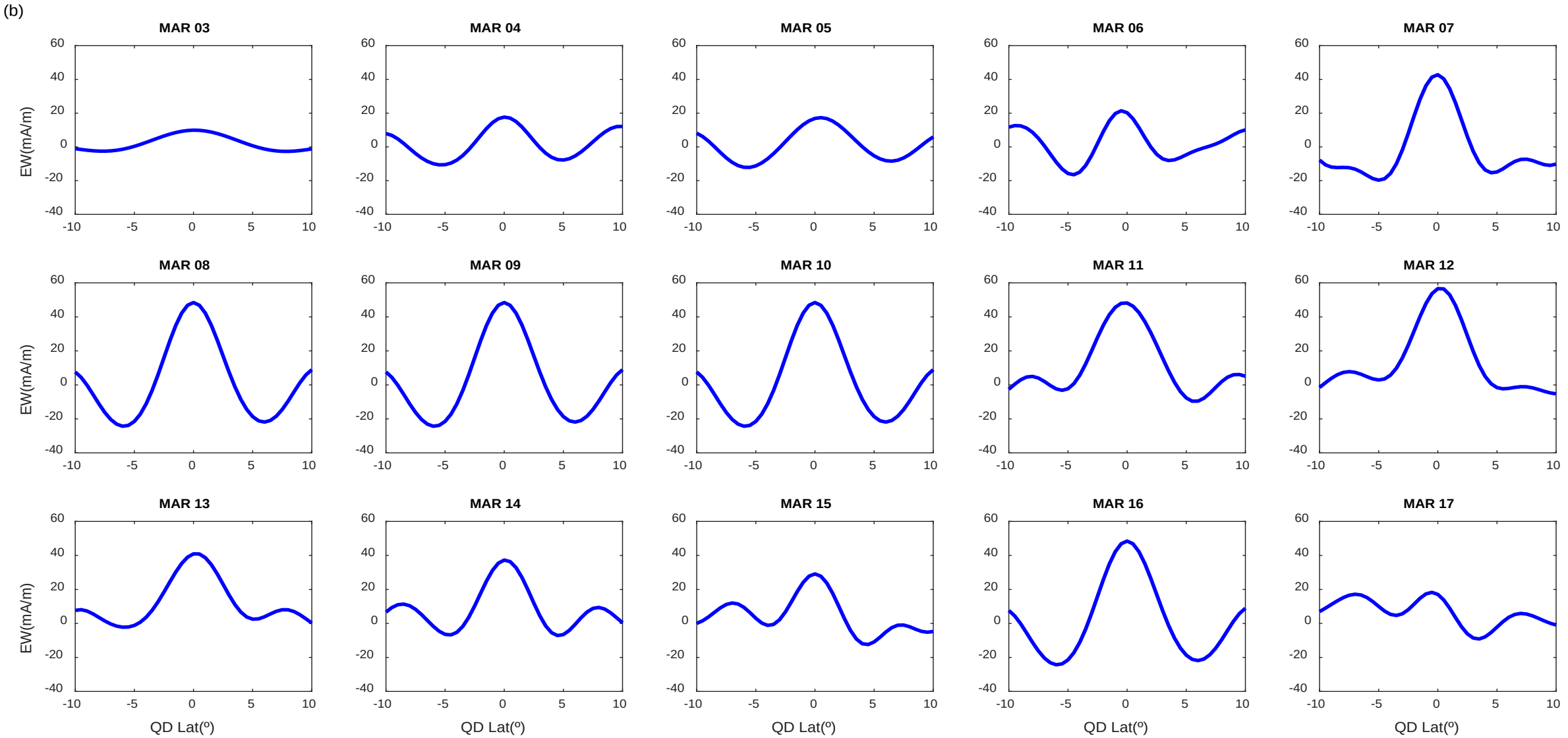

Figure 11: Day-to-day variations in eastward (EW) current density profile from 3–17th March, 2014: (b) American sector

Conclusions

1. In addition to the roles played by geomagnetic storms and other solar events in space weather, lower atmospheric couplings also play significant roles, particularly in the ionospheric part of space weather.

2. Reversal of the stratospheric zonal mean wind direction supported the formation of a reversed fountain effect in both sectors.

3. TEC generally recorded higher intensity in the American sector than in the African sector. From the PPEF, EEJ, and inferred vertical drift data, ionospheric electrodynamics over the American sector during the period of investigation was higher than that of the African sector.

4. Over the American sector the major SSW forcing weakens irregularities on March 15 and 21–23

REFERENCE

Idolor, O. R, Akala, A. O & Bolaji, O. S (2021), Responses of the African and American Equatorial Ionization Anomaly (EIA) to 2014 arctic SSW events, *Space weather*, DOI:10.1029/2021SW002812

Thanks For Listening